Modeling and simulation of a grand piano.

Juliette Chabassier, Antoine Chaigne, Patrick Joly

Modeling and simulation of a grand piano.

Juliette Chabassier, Antoine Chaigne, Patrick Joly

RESEARCH REPORT
N° 8181
December 2012
Project-Teams Poems and Magique3d

ISSN 0249-6399 ISRN INRIA/RR--8181--FR+ENG

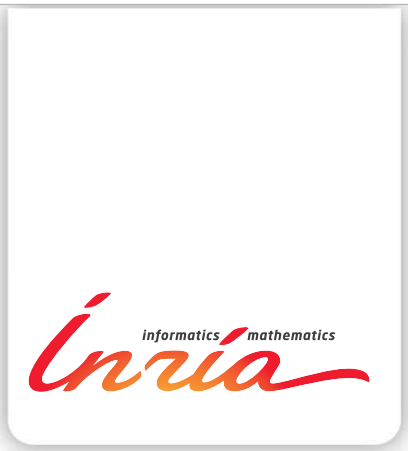

Modeling and simulation of a grand piano.

Juliette Chabassier*†, Antoine Chaigne‡, Patrick Joly †

Project-Teams Poems and Magique 3d

Research Report n° 8181 — December 2012 — 28 pages

* Magique 3d team
† Poems team
‡ UME Ensta

RESEARCH CENTRE
BORDEAUX – SUD-OUEST

200 Avenue de la Vieille Tour,
33405 Talence Cedex

Abstract: The purpose of this study is the time domain modeling and numerical simulation of a piano. We aim at explaining the vibratory and acoustical behavior of the piano, by taking into account the main elements that contribute to sound production. The soundboard is modeled as a bidimensional thick, orthotropic, heterogeneous, frequency dependant damped plate, using Reissner Mindlin equations. The vibroacoustics equations allow the soundboard to radiate into the surrounding air, in which we wish to compute the complete acoustical field around the perfectly rigid rim. The soundboard is also coupled to the strings at the bridge, where they form a slight angle from horizontal. Each string is modeled by a one dimensional damped system of equations, taking into account not only the transversal waves excited by the hammer, but also the stiffness thanks to shear waves, as well as the longitudinal waves arising from geometric nonlinearities. The hammer is given an initial velocity that projects it towards a choir of strings, before being repelled. The interacting force is a nonlinear function of the hammer compression.
The final piano model that will be discretized is a coupled system of partial differential equations, each of them exhibiting specific difficulties (nonlinear nature of the string system of equations, frequency dependant damping of the soundboard, great number of unknowns required for the acoustic propagation), in addition to couplings' inherent difficulties. On the one hand, numerical stability of the discrete scheme can be compromised by nonlinear and coupling terms. A very efficient way to guarantee this stability is to construct a numerical scheme which ensures the conservation (or dissipation) of a discrete equivalent of the continuous energy, across time steps. A major contribution of this work has been to develop energy preserving schemes for a class of nonlinear systems of equations, in which enters the string model. On the other hand, numerical efficiency and computation time reduction require that the unknowns of each problem's part, for which time discretization is specific, hence different, be updated separately. To achieve this artificial decoupling, adapted Schur complements are performed after Lagrange multipliers are introduced. The potential of this time domain piano modeling is emphasized by realistic numerical simulations. Beyond greatly replicating the measurements, the program allows us to investigate the influence of physical phenomena (string stiffness or nonlinearity), geometry or materials on the general vibratory behavior of the piano, sound included. Spectral enrichment, "phantom partials" and nonlinear precursors are clearly revealed when large playing amplitudes are involved, highlighting how this approach can help better understand how a piano works.

Key-words: piano, modeling, energy, nonlinear precursor, phantom partials, damping phenomena

Modélisation et simulation numérique d'un piano à queue.

Résumé : Cette étude porte sur la modélisation et la simulation numérique d'un piano, en domaine temporel, par modèles physiques. Nous souhaitons rendre compte du comportement vibratoire et acoustique du piano, en prenant en compte les éléments principaux qui contribuent à la production du son. La table d'harmonie est modélisée par une équation bidimensionnelle de plaque épaisse, le système de Reissner Mindlin, pour un matériau orthotrope et hétérogène, dont l'amortissement dépend de la fréquence. Grce aux équations de la vibroacoustique, la table rayonne dans l'air, dans lequel on souhaite calculer le champ acoustique complet autour de la ceinture du piano, que l'on suppose rigide. La table d'harmonie est d'autre part sollicitée par les cordes, à travers le chevalet o elles présentent un léger angle par rapport au plan horizontal. Chaque corde est modélisée par un système d'équations monodimensionnelles amorties dans lequel on prend en compte non seulement les ondes transversales excitées par le marteau, mais aussi la raideur à travers les ondes de cisaillement, ainsi que le couplage avec les ondes longitudinales provenant de la prise en compte des non linéarités géométriques. Le marteau est lancé avec une vitesse initiale vers un chœur de cordes, contre lequel il s'écrase avant d'tre repoussé par les cordes. La force d'interaction dépend de façon non linéaire de l'écrasement du marteau.

Le modèle complet de piano, que l'on souhaite résoudre numériquement, consiste donc en un système couplé d'équations aux dérivées partielles, dont chacune revt des difficultés de nature différente : la corde est régie par un système d'équations non linéaires, la table d'harmonie est soumise à un amortissement dépendant de la fréquence, la propagation acoustique requiert un très grand nombre d'inconnues ; auxquelles s'ajoute la difficulté inhérente aux couplages. D'une part, la stabilité numérique du schéma discret peut tre compromise par la présence d'équations non linéaires et de nombreux couplages. Une méthode efficace pour garantir cette stabilité a priori est de construire un schéma qui conserve, ou dissipe, un équivalent discret de l'énergie physique d'un pas de temps au suivant. Une contribution majeure de ce travail a été de développer des schémas préservant une énergie discrète pour une classe de systèmes non linéaires dans laquelle s'inscrit le modèle de corde. D'autre part, afin d'augmenter l'efficacité de la méthode et de réduire le coût des calculs numériques, il est souhaitable de mettre à jour de façon découplée les inconnues liées aux différentes parties du problème, sur lesquelles la discrétisation en temps est faite de façon différente, afin de s'adapter aux spécificités de chacune. L'introduction de multiplicateurs de Lagrange nous permet de réaliser ce découplage artificiel grce à des compléments de Schur adaptés.

L'utilisation du code de calcul en situation réaliste montre le potentiel d'une telle modélisation d'un piano complet en domaine temporel. Au delà de très bien reproduire les mesures, il est possible d'étudier l'influence de certains phénomènes physiques (corde raide, non linéaire), de la géométrie ou encore des matériaux utilisés sur le comportement vibratoire général du piano, et sur le son en particulier. L'enrichissement spectral, ainsi que l'apparition des "partiels fantômes" et du précurseur non linéaire sont clairement mis en évidence pour les grandes amplitudes de jeu, soulignant l'intért de notre approche dans la compréhension du fonctionnement de l'instrument.

Mots-clés : piano, modélisation, énergie, précurseur non linéaire, partiels fantômes, phénomènes d'amortissement

1 Introduction

In this paper, an extensive and global model of a piano is presented. Its aim is to reproduce the main vibratory and acoustic phenomena involved in the generation of a piano sound from the initial blow of the hammer against the strings to the radiation from soundboard to the air. Compared to previous studies, one first originality of the work is due to the string model which takes both geometrical nonlinear effects and stiffness into account. Other significant improvements are due to the combined modeling of the three main couplings between the constitutive parts of the instrument: hammer-string, string-soundboard and soundboard-air coupling.

Although a vast literature exist on the piano and its subsystems (strings, hammer, soundboard, radiated field), there are only a few examples of a complete computational model of the instrument. One noticeable exception is the work by Giordano and Jiang [Giordano and Jiang, 2004] describing the modeling of a linear string coupled to soundboard and air using finite differences. Compared to this reference, our work is based on a more accurate description of the piano physics, and also put more attention to the properties of the numerical schemes used for solving the complex system of coupled equations. The strategy used here for the piano is similar to the one developed previously by two of the authors for the guitar [Derveaux et al., 2003] and the timpani [Rhaouti et al., 1999]. The physical model is composed of a set of equations governing the hammer-string contact and the wave propagation in strings, soundboard and air, in the time domain. The input parameters of the equations are linked to the geometry and material properties of the propagation media. The equations are then discretized in time and space, in order to allow the numerical resolution of the complete system. Original numerical schemes are developed in order to ensure stability, sufficient accuracy and the conservation of energy. In this respect, this strategy has a direct continuity with the work by Bilbao [Bilbao, 2005].

The numerical dispersion of the schemes is maintained sufficiently small so that the difference between real and simulated frequencies are comparable to the just noticeable differences of the human ear in the audible range (around 1 %). The validity of the numerical model is assessed by careful analysis, in time and frequency, of the most significant variables of the problem: hammer force, string, bridge and soundboard displacements (resp. velocities or accelerations), sound pressure. In a first step, using typical values of parameters found in the literature, the numerical results are expected to reproduce the main features of piano sounds, at least qualitatively. In a second step, the input parameters are the results of measurements on real pianos, and a more thorough comparison is made between real and simulated tones.

One motivation at the origin of this study was to reproduce the effects of the geometrical nonlinearity of piano strings both in time (precursors[Askenfelt, 1993], transverse-longitudinal coupling) and frequency domain (phantom partials[Harold A. Conk
The purpose of the simulations is to get a better understanding of these phenomena: the aim is to exhibit quantitative links between some control parameters (initial hammer velocity, string tension,...) and observed waveforms and spectra. Experimental observations of string and soundboard spectra recorded on real pianos suggest, in addition, that the string-soundboard coupling plays a crucial role in the transmission of longitudinal string components [Giordano and Korty, 1996], and thus attempting to reproduce and understand these effects is another challenge.

In pianos, it is well-known that the initial transients are perceptually highly significant. One major attribute of spectral content during the attack is due to the presence of soundboard modes excited by the string force at the bridge. The low-frequency modes, in particular, have low damping: they are well separated and clearly recognizable on the spectra [Harold A. Conklin, 1996a]. An accurate model of string-soundboard coupling has the capability of accounting for such effects. Soundboard modeling also allows to explore the effects of bridge and ribs distribution on the produced sound.

Finally, air-soundboard coupling is a necessary step for simulating sound pressure. Because of the wideband modeling, the computation of a 3-D pressure field is highly demanding. High performance parallel computing was necessary here. However, the results are very valuable, since one can make direct auditory comparisons with real piano sounds. Simulation of a 3-D field also yields information on directivity and sound power.

The physical model of the piano used in this work is presented in Section 2. Emphasis is put on what we believe to be the most significant innovative parts of the model: the nonlinear stiff string and its coupling with an heterogeneous orthotropic soundboard via the bridge. Hammer-string interaction and air-soundboard coupling are also described. In Section 3, the general method used for putting the model into a discrete form is explained. The properties of the main numerical schemes retained for each constitutive part of the instrument and the coupling conditions are given without demonstrations, with explicit references to other papers published by the authors, that are more oriented on the mathematical aspects of the model.

The validity of the model is evaluated in Section 4 through analysis of a selection of simulated piano notes in the low, medium and treble register, respectively. The motion of the main elements (piano hammer, strings, bridge, soundboard, air) are analyzed alternatively in time, space, and/or frequency domain. Because of the important effort put on the nonlinear string, the capability of the model to reproduce amplitude-dependent phenomena is particularly emphasized.

Comparisons are also made with measurements performed on a Steinway grand piano (D model). In these series of experiments, the motion of hammer, string, bridge and soundboard, and the sound pressure were recorded simultaneously. This shed useful light on the transmission and transformation of the signals from hammer to sound and, through comparisons, on the ability of the model to account for the coupling between the constitutive parts of the piano.

2 Presentation of the model

The goal of the work is to develop a physical model of the piano in the time domain that accounts for the main vibratory and acoustical functions of the instrument. A relatively high degree of accuracy is required in the physical description so that relevant links can be established between the parameters of the model and instrument making. Because of the complexity of the model, no analytical solution can be expected, and numerical simulations must be conducted. Therefore, another requirement of the work is to develop an accurate numerical formulation of the problem. During the development of the model, particular attention was paid to the following guidelines:

- The prime function of the piano is to generate sounds. However, its conception is not only governed by dynamical and acoustical laws, but also by purely static and mechanical considerations, as it is the case, for example, for the design of frame, rim and feet. In addition, from the point of view of the player, the piano must fulfill a number of playability rules. Our purpose is not to mimic piece by piece the construction of a real instrument, but rather to describe the major phenomena that are at the origin of piano tones. This is achieved here by considering a set of equations governing the nonlinear hammer-string contact, the wave propagation in strings, the vibrations of the heterogeneous orthotropic soundboard radiating in air, and the reciprocal coupling between strings and soundboard at the bridge.

- Several simplifying assumptions were made in the model. The hammer is supposed to be perfectly aligned with the strings. The agraffe is assumed to be rigidly fixed with a simply supported end condition for the strings. Both the string-soundboard and soundboard-air couplings are lossless. The soundboard is considered as simply supported along its edge, and the "listening" room is anechoic with no obstacle except the piano itself. Finally, the action of the mechanism prior to the shock of the hammer against the strings is ignored. In other words, the tone starts when the hammer hits the strings with an imposed velocity.

- Most of the physical parameters of hammers, strings and soundboards included in the model are obtained from standard string scaling and geometrical data from piano, strings and soundboards manufacturers. When necessary, these data were complemented by results of our own measurements on various instruments. However, some difficulties arose for the physical description of damping models in hammers, strings and soundboards since the underlying physical mechanisms are often very complex, and because an accurate analytical description of these phenomena are not available in the present state-of-the-art. Thus, it was decided to use here approximate models based on experimental data, as it is commonly done in other fields of structural dynamics [Balmes, 2006].

- As shown in Section 3, the numerical formulation of the model is based on a discrete formulation of the global energy of the system, which ensures stability. This requires, first, that the continuous energy of the problem is decaying with time. The global model of the piano is thus written according to this condition.

In what follows, an energy decaying model is developed for each constitutive part of the instrument, successively. Finally, a global piano model is proposed.

2.1 Strings

The selected string model accounts for large deformations, inducing geometrical nonlinearities, and intrinsic stiffness. These are two essential physical phenomena in piano strings [Jarvelainen et al., 2001, Bank and Lehtonen, 2010]. The governing equations correspond to those of a Timoshenko beam under axial tension. Modeling the stiffness with a Timoshenko model, rather than with an Euler-Bernoulli model as in [Chaigne and Askenfelt, 1994], is motivated by both physical and numerical reasons. As shown in Section 4 below, the physical dispersion predicted by the Timoshenko model shows a good agreement with experimental data in a wider frequency range than the Euler-Bernoulli model. It also yields an asymptotic value for the transverse wave velocity as the frequency increases, in contrast with the Euler-Bernoulli model. This latter property is not only more satisfying from the point of view of the physics, but it is also more tractable in the simulations. The geometrical nonlinearities are described using a standard model[Morse and Ingard, 1968].

Let us call ρ the density of the string, A the area of its cross-section, T_0 its tension at rest, E its Young's modulus, I its stiffness inertia coefficient, G its shear coefficient, and κ the nondimensional Timoshenko parameter. We denote $u_s(x,t)$ the transverse vertical displacement, $v_s(x,t)$ the longitudinal displacement, and $\varphi_s(x,t)$ the angle of the cross-sections with the plane normal to the string. The space variable is $x \in [0, L]$, where L is the length of the string at rest (see Figure 1). For the end conditions, we assume zero displacement (in both transverse and longitudinal directions) and zero moment. These conditions are motivated by usual observations at the agraffe ($x = 0$) [Harold A. Conklin, 1996b], and will be revisited later at point $x = L$ when considering the coupling with the soundboard. Finally, we consider that the string is at rest at the origin of time. We get the following system (1), where S is a source term. As shown in the next paragraph, this term is supposed to account for the action of the hammer against the strings. The model is written:

String motion: (1)

$$\begin{cases} \rho A \dfrac{\partial^2 u_s}{\partial t^2} - \dfrac{\partial}{\partial x}\left[EA\dfrac{\partial u_s}{\partial x} - \dfrac{(EA - T_0)\dfrac{\partial u_s}{\partial x}}{\sqrt{\left(\dfrac{\partial u_s}{\partial x}\right)^2 + \left(1 + \dfrac{\partial v_s}{\partial x}\right)^2}} \right] + AG\kappa \dfrac{\partial}{\partial x}\left(\varphi_s - \dfrac{\partial u_s}{\partial x}\right) = S, \\ \rho A \dfrac{\partial^2 v_s}{\partial t^2} - \dfrac{\partial}{\partial x}\left[EA\dfrac{\partial v_s}{\partial x} - \dfrac{(EA - T_0)\left(1 + \dfrac{\partial v_s}{\partial x}\right)}{\sqrt{\left(\dfrac{\partial u_s}{\partial x}\right)^2 + \left(1 + \dfrac{\partial v_s}{\partial x}\right)^2}} \right] = 0, \\ \rho I \dfrac{\partial^2 \varphi_s}{\partial t^2} - EI\dfrac{\partial^2 \varphi_s}{\partial x^2} + AG\kappa \left(\varphi_s - \dfrac{\partial u_s}{\partial x}\right) = 0 \end{cases}$$

Boundary conditions: (2)

$$u_s(x = x_b, t) = v_s(x = x_b, t) = \frac{\partial \varphi_s}{\partial x}(x = x_b, t) = 0, \qquad \text{for } x_b \in \{0, L\},$$

Initial conditions: (3)

$$\begin{cases} u_s(x, t = 0) = v_s(x, t = 0) = \varphi_s(x, t = 0) = 0, \\ \dfrac{\partial u_s}{\partial t}(x, t = 0) = \dfrac{\partial v_s}{\partial t}(x, t = 0) = \dfrac{\partial \varphi_s}{\partial t}(x, t = 0) = 0. \end{cases}$$

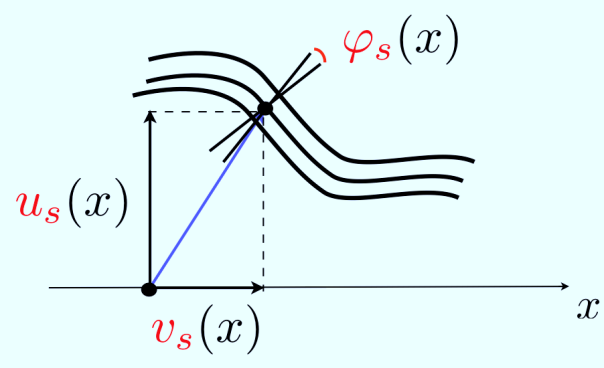

Figure 1: Schematic view of the string motion with the three variables: flexural displacement $u_s(x,t)$, longitudinal displacement $v_s(x,t)$, shear angle $\varphi_s(x,t)$. (Color online)

The eigenfrequencies of the linearized version of (1)-(2) can be computed analytically (see, for example[Chabassier and Imperiale, 201 which yield three different series. The following expressions hold for partial's rank $\ell \geq 1$. The flexural eigenfrequencies are given by:

$$f_\ell^{trans} = \ell f_0^{trans}\left(1+\epsilon\,\ell^2\right)+\mathcal{O}(\ell^5), \quad \text{where } f_0^{trans} = \frac{1}{2L}\sqrt{\frac{T_0}{\rho A}}, \quad \epsilon = \frac{\pi^2}{2L^2}\frac{EI}{T_0}\Big[1-\frac{T_0}{EA}\Big]. \tag{4}$$

The shear eigenfrequencies satisfy:

$$f_\ell^{shear} = f_0^{shear}\left(1+\eta\,\ell^2\right)+\mathcal{O}(\ell^4), \quad \text{where } f_0^{shear} = \frac{1}{2\pi}\sqrt{\frac{AG\kappa}{\rho I}}, \quad \eta = \frac{\pi^2}{2L^2}\frac{EI+IG\kappa}{AG\kappa}. \tag{5}$$

These shear frequencies, which are situated well above the audio range, are not perceived by the human ear. Finally, the longitudinal eigenfrequencies read

$$f_\ell^{longi} = \ell f_0^{longi}, \quad \text{where } f_0^{longi} = \frac{1}{2L}\sqrt{\frac{E}{\rho}}. \tag{6}$$

Equation (4) shows that the model accounts for inharmonicity. The inharmonicity coefficient ϵ is close to, but slightly different from, the usual coefficient obtained with the Euler-Bernoulli model[Fletcher, 1964]. The speed of waves associated to equations (4) and (6) are the transverse speed $c^{trans} = \sqrt{T_0/\rho A}$ and the longitudinal speed $c^{longi} = \sqrt{E/\rho}$. For the string C2, for example, we obtain $c^{trans} = 209$ m·s^{-1} and $c^{longi} = 5840$ m·s^{-1}. If both types of waves are present on the string (which is the case because of nonlinear transverse to longitudinal coupling), the speed ratio explains why the longitudinal waves arrive first at the bridge, inducing a precursor.

With the objective to simulate realistic tones, it is essential to account for the observed frequency dependent damping on strings. Damping phenomena in structures in general, and in strings in particular, are hard to apprehend, for many reasons (lack of available measurements, uneasy separation of the mechanisms, difficulty in modeling microscale phenomena such as dislocations, in the equation of motion,...). Therefore, following the strategy used by a number of previous authors, we use a simple model that globally and approximately accounts for the damping effect, without pretending to model the underlying physics in details [Bensa et al., 2003]. In practice, viscoelastic terms are added under the form:

$$2\,\rho A\,R_u\,\frac{\partial u_s}{\partial t} - 2\,T_0\,\eta_u\frac{\partial^3 u_s}{\partial t\,\partial x^2} \tag{7}$$

where R_u (in s) and η_u (in s^{-1}) are empirical damping coefficients to be determined from measured sounds for each string, through comparisons between simulated and measured spectrograms. Similar damping terms have to be added for shear and longitudinal motions in order to avoid unpleasant endless frequencies in the simulated tones.

$$2\,\rho A\,R_v\,\frac{\partial v_s}{\partial t} - 2\,EA\,\eta_v\frac{\partial^3 v_s}{\partial t\,\partial x^2}, \qquad 2\,\rho I\,R_\varphi\,\frac{\partial \varphi_s}{\partial t} - 2\,EI\,\eta_\varphi\frac{\partial^3 \varphi_s}{\partial t\,\partial x^2} \tag{8}$$

Again, the order of magnitude for (R_v, R_φ) and (η_v, η_φ) are determined from experiments and/or trial-and-error procedures, considering the absence of any other reliable method.

When the system is subjected to a source term $S(x,t)$ in the transverse direction, it is possible to show the following energy identity [Chabassier et al., 2012a]:

$$\begin{aligned}
&\frac{d\mathcal{E}_s}{dt} \leq \int_0^L S\,\frac{\partial u_s}{\partial t} \qquad \text{where } \mathcal{E}_s(t) = \mathcal{E}_{s,kin}(t) + \mathcal{E}_{s,pot}(t) \qquad (9)\\
&\mathcal{E}_{s,kin}(t) = \frac{\rho A}{2}\int_0^L\left(\frac{\partial u_s}{\partial t}\right)^2 + \frac{\rho A}{2}\int_0^L\left(\frac{\partial v_s}{\partial t}\right)^2 + \frac{\rho I}{2}\int_0^L\left(\frac{\partial \varphi_s}{\partial t}\right)^2\\
&\mathcal{E}_{s,pot}(t) = \frac{T_0}{2}\int_0^L\left(\frac{\partial u_s}{\partial x}\right)^2 + \frac{EA}{2}\int_0^L\left(\frac{\partial v_s}{\partial x}\right)^2 + \frac{EI}{2}\int_0^L\left(\frac{\partial \varphi_s}{\partial x}\right)^2 + \frac{AG\kappa}{2}\int_0^L\left(\frac{\partial u_s}{\partial x}-\varphi_s\right)^2\\
&\qquad\qquad + (EA-T_0)\int_0^L\left[\frac{1}{2}\left(\frac{\partial u_s}{\partial_x}\right)^2 + \left(1+\frac{\partial v_s}{\partial x}\right) - \sqrt{\left(\frac{\partial u_s}{\partial x}\right)^2 + \left(1+\frac{\partial v_s}{\partial x}\right)^2}\right]
\end{aligned}$$

This quantity is always positive in practice since, for real piano strings, we have $EA > T_0$. Advantage of this property will be taken to derive stable numerical schemes for solving the nonlinear system of equations.

2.2 Hammer

We now turn to the interaction between the hammer and the strings. Depending on the note, the hammer strikes one, two or three strings. The components of the motion of the i*th* string's of a given note's set are written $(u_{s,i}, v_{s,i}, \varphi_{s,i})$. Since the strings belonging to the same note are slightly detuned[Weinreich, 1977], each string has a different tension at rest $T_{0,i}$ in (1). The hammer's center of gravity is supposed to be moving along a straight line orthogonal to the strings at rest. Its displacement on this line is represented by $\xi(t)$. The interaction force between the hammer and the i*th* string of a note is distributed on a small portion of the string, through a spreading function $\delta^{\mathcal{H}}$ (represented in figure 2) localized around the impact point, with $\displaystyle\int_0^L \delta^{\mathcal{H}}(x)\,dx = 1$, and oriented in the transversal direction.

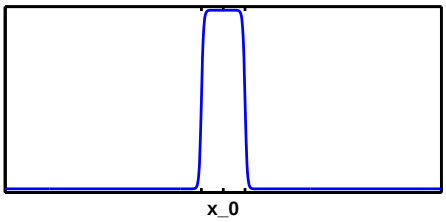

Figure 2: Spreading function $\delta^{\mathcal{H}}(x)$ used to model the hammer string contact.

As a consequence, we denote $\langle u_{s,i}\rangle$ the weighted average of the transverse displacement of the string:

$$\langle u_{s,i}\rangle(t) = \int_0^L u_{s,i}(x,t)\,\delta^{\mathcal{H}}(x)\,dx. \tag{10}$$

The interaction force depends on the distance $d(t)$ between the hammer and the string: if $d(t) > \overline{\xi}$, there is no contact and the force is zero. If $d(t) \leq \overline{\xi}$, the force is a function of the distance. According to previous studies, we define the function:

$$\Phi(d) = \Big[\big(\overline{\xi} - d\big)^+\Big]^p \tag{11}$$

where $(\cdot)^+$ means "positive part of", and where p is a real positive nonlinear exponent. In practive, this coefficient varies between 1.5 and 3.5 [Stulov, 2004, Giordano and II, 2000, Chaigne and Askenfelt, 1994]. In order to account further for the observed hysteretic behavior of the felt[Stulov, 2004], a dissipative term is added in the expression of the force. In summary, the parameters characterizing the mechanical behavior of the hammer are its equivalent mass $M^{\mathcal{H}}$, its stiffness coefficient $K_i^{\mathcal{H}}$ and its dissipation coefficient $R_i^{\mathcal{H}}$. The index i here indicates that the model can eventually account for the fact that the interaction with hammer might not be uniform for each string of a note. The interacting force between the hammer and the i*th* string finally reads

$$F_i^{\mathcal{H}}(t) = K_i^{\mathcal{H}}\Phi\big(\langle u_{s,i}\rangle(t) - \xi(t)\big) + R_i^{\mathcal{H}}\frac{d}{dt}\Phi\big(\langle u_{s,i}\rangle(t) - \xi(t)\big). \tag{12}$$

The hammer is submitted to the sum of these forces. Conversely, the right hand side $S(x,t)$ of the strings system (1) is replaced with $F_i^{\mathcal{H}}(t)\,\delta^{\mathcal{H}}(x)$.
We consider an initial position $-\xi_0$ and an initial velocity $v_0^{\mathcal{H}}$ for the hammer, while the strings are considered at rest at the origin of time. Defining further $\Psi(d) = \displaystyle\int_d^{+\infty} \Phi(s)\,ds$ One can show (see Chabassier *et al.*[Chabassier et al., 2012a]) that any regular solution to the resulting hammer – strings system satisfies the following energy decay:

$$\frac{d\mathcal{E}_{s,h}}{dt} \leq 0, \text{ with } \quad \mathcal{E}_{s,h}(t) = \sum_i \Big[\mathcal{E}_{s,i}(t) + K_i^{\mathcal{H}}\Psi\big(\langle u_{s,i}\rangle(t) - \xi(t)\big)\Big] + \frac{M^{\mathcal{H}}}{2}\Big(\dot{\xi}(t)\Big)^2 \geq 0 \tag{13}$$

where $\mathcal{E}_{s,i}(t)$ is the energy defined in (9) for the i*th* string.

2.3 Soundboard

The only vibrating element of the piano case considered in the model is the soundboard, all other parts (rim, keybed, lid, iron frame...) being assumed to be perfectly rigid. In view of the small "thickness over other dimensions" ratio of the piano soundboard, a bidimensional Reissner-Mindlin plate model is considered. This model is the bidimensional equivalent to the linear Timoshenko model. It has been preferred here to the Kirchhoff-Love model, because its yields a better estimate for the soundboard motion, in the complete audio range. It also has better mathematical properties [Chabassier et al., 2012a]. The variables of the motion are the vertical transverse displacement $u_p(x, y, t)$ at a current point of coordinates (x, y) of the bidimensional plate ω, and two shear angles $\theta_{x,p}(x, y, t)$ and $\theta_{y,p}(x, y, t)$. These last two variables account for the deviation of the straight segments of the plate from the normal to the medium surface, in the $(\underline{e}_x, \underline{e}_y)$-referential plane (see Figure 3). The vector $\underline{\theta}_p(x, y, t)$ groups these two angles. The bridge and ribs are considered as heterogeneities of the soundboard, and the orientation of the orthotropy axes can be space dependent. As a consequence, the physical coefficients representing the density ρ, the thickness δ, the Young's moduli in the two main directions of orthotropy E_x and E_y, the shear moduli in the three main directions of orthotropy G_{xy}, G_{xz} and G_{yz}, the Poisson's ratios ν_{xy} and ν_{yx}, and the shear coefficient κ_x and κ_y are functions of space.

Modeling the thickness as a space dependent variable accounts for a diaphragmatic soundboard [Bilhuber and Johnson, 1940] (the thickness varies between 6 and 9 mm in the soundboard, between 9 and 35 mm on the ribs, between 29 and 69 mm on the bridge, and between 29 and 95 mm on the crossing areas of ribs and bridge, in the proportions shown qualitatively in Figure 3(b) and (c)). The soundboard is assumed to be simply supported[Mamou-Mani et al., 2008] on its edge $\partial\omega$. Finally, a source term is imposed in the transverse vertical direction. The function of this term is to account for both the string's tension at the bridge (see 2.4) and the air pressure jump (see 2.5).

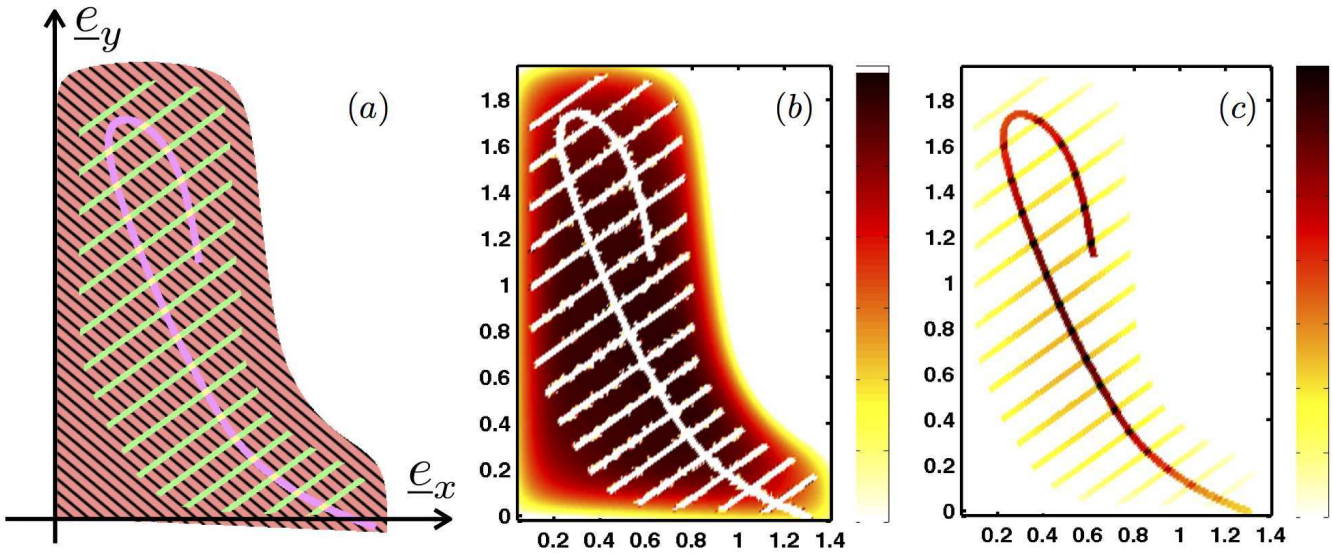

Figure 3: (a) Schematic view of the four different zones of the soundboard in the referential plane. The angle of orthotropy is -40 degrees with the vector $\underline{e}_x$ in the plate (directed along the stripes), bridge and crossing zones, and is 54 degrees in the ribs zone (along the ribs direction). (b) Variable thickness on the plate, where the darkest areas are the thickest. (c) Variable thickness of ribs and bridge. (Color online)

For simplicity, the possible rotation of the orthotropy axes in the soundboard is ignored in the presentation, although it is considered in the model and the numerical simulations. In this case, the Reissner-Mindlin system that governs the

	ρ kg·m^{-3}	E_x GPa	E_y GPa	G_{xy} GPa	G_{xz} GPa	G_{yz} GPa	ν_{xy} -
Spruce	380	11.0	0.650	0.66	1.2	0.042	0.26
Beech	750	13.7	2.24	1.61	1.06	0.46	0.3

Table 1: Parameters used for the wooden soundboard: Spruce for the table and the ribs, Beech for the bridge.

motion of transverse displacement and shear angles is written for (x, y) belonging to the 2d domain ω:

$$\begin{cases} \rho\,\dfrac{\delta^3}{12}\dfrac{\partial^2\underline{\theta}_p}{\partial t^2} - \underline{\mathrm{Div}}\left(\dfrac{\delta^3}{12}\,\mathbf{C}\,\underline{\varepsilon}(\underline{\theta}_p)\right) + \delta\,\underline{\kappa}^2\cdot\underline{G}\cdot(\underline{\nabla}u_p + \underline{\theta}_p) = 0 & \text{(14a)} \\ \rho\,\delta\dfrac{\partial^2 u_p}{\partial t^2} - \mathrm{div}\left(\delta\,\underline{\kappa}^2\cdot\underline{G}\cdot(\underline{\nabla}u_p + \underline{\theta}_p)\right) = f & \text{(14b)} \\ u_p = \mathbf{C}\underline{\varepsilon}(\underline{\theta}_p)\,\underline{n} = 0 \qquad \text{on } \partial\omega & \text{(14c)} \end{cases}$$

$$\text{with}\mathbf{C}\ \underline{\varepsilon} = \begin{pmatrix} \dfrac{E_x}{1-\nu_{xy}\nu_{yx}} & -\dfrac{E_y\nu_{xy}}{1-\nu_{xy}\nu_{yx}} & 0 \\ -\dfrac{E_x\nu_{yx}}{1-\nu_{xy}\nu_{yx}} & \dfrac{E_y}{1-\nu_{xy}\nu_{yx}} & 0 \\ 0 & 0 & 2G_{xy} \end{pmatrix} \begin{pmatrix} \varepsilon_{xx} \\ \varepsilon_{yy} \\ \varepsilon_{xy} \end{pmatrix} \text{ where the tensor } \underline{\varepsilon} \text{ is symmetric,} \qquad (15)$$

$$\underline{G} = \begin{pmatrix} G_{xz} \\ G_{yz} \end{pmatrix}, \quad \underline{\kappa}^2 = \begin{pmatrix} \kappa_x^2 \\ \kappa_y^2 \end{pmatrix}.$$

Here, $\underline{\mathrm{Div}}$ is the divergence operator for tensors: $\underline{\mathrm{Div}}(\tau) = \partial_j \tau_{i,j}$, $\underline{\varepsilon}$ it the linearized strain tensor, div and $\underline{\nabla}$ are the divergence and gradient operators for $\mathbb{R}^2$ vectors. Table 1 gives the parameters used for the soundboard wood (Spruce for the table and the ribs, Beech for the bridge). A prestress term could be added to this model, accounting for the static action of the strings on the curved soundboard. Since this action contributes to reduce the initial crown of the soundboard in such a way that it becomes almost flat in normal use, the curvature of the soundboard is ignored here.

With regard to the modeling of damping in the soundboard material, a modal approach has been adopted where the modal damping can be adjusted, mode by mode. This method is justified as long as the damping factor is small compared to the eigenfrequency, and is of current use in structural dynamics [Hasselman, 1976]. This procedure also requires that the modes are sufficiently well separated, a condition that is only valid here below 1 to 2 kHz[Ege, 2012]. The modal amplitudes $X_n(t)$ on the nth mode associated to the frequency f_n are then solution of the second-order uncoupled damped oscillators equations:

$$\frac{d^2X_n}{dt^2} + \alpha(f_n)\frac{dX_n}{dt} + (2\pi f_n)^2\,X_n = F_n \qquad (16)$$

where α is a positive damping function, whose value is associated to each eigenmode, and derived from experiments [Ege, 2012], and F_n is the modal contribution of the transversal source term f.

For any positive damping law it is possible to show the following energy identity:

$$\begin{aligned} &\frac{d\mathcal{E}_p}{dt} \le \iint_\omega f\,\frac{\partial u_p}{\partial t} \qquad \text{where } \mathcal{E}_p(t) = \mathcal{E}_{p,kin}(t) + \mathcal{E}_{p,pot}(t) \qquad (17) \\ &\mathcal{E}_{p,kin}(t) = \iint_\omega \rho\,\delta\,\left(\frac{\partial u_p}{\partial t}\right)^2 + \iint_\omega \rho\frac{\delta^3}{12}\left|\frac{\partial\underline{\theta}_p}{\partial t}\right|^2 \\ &\mathcal{E}_{p,pot}(t) = \iint_\omega \frac{\delta^3}{12}\mathbf{C}\,\underline{\varepsilon}(\underline{\theta}_p) : \underline{\varepsilon}(\underline{\theta}_p) + \iint_\omega \delta\,\underline{\kappa}^2\cdot\underline{G}\,|\underline{\nabla}u_p + \underline{\theta}_p|^2 \end{aligned}$$

Thus, like for the strings-hammer system, we can conclude that the energy of the soundboard decays with time, after extinction of the source.

2.4 Strings-soundboard coupling at the bridge

The main purpose of the bridge is to transmit the vibrations of the strings to the soundboard. As highlighted by the spectral content of the precursor signal[Podlesak and Lee, 1988], it is essential to model the transmission of both transverse and longitudinal waves of the string to the rest of the structure. The literature is not very broad concerning this part of the instrument, with a few exceptions [Giordano and Korty, 1996, Cuenca and Caussé, 2007]. Also few experimental data are available and the wave transmission phenomena occurring at the bridge are still not clearly understood. For these reasons, we decided to describe a plausible, though not fully proved, way for the transformation of string longitudinal motion to bridge transverse motion. It is based on the observation that the strings form a slight angle α with the horizontal plane due to both bridge height and soundboard curvature. We also assume that the bridge moves in the vertical direction. This, again, seems to be a reasonable assumption since the static tension of the complete set of strings prevents the bridge motion to have a significant component parallel to the strings. At this point, we are aware of the fact that some authors were able to identify and measure such a component [Giordano and Korty, 1996], but we must admit that we were no able to exhibit similar features in our measurements. It would be probably also necessary in the future to revisit the assumption of ignoring the horizontal bridge motion perpendicular to the strings, that might induce an horizontal component to the string motion.

When the hammer strikes the strings, it gives rise to a transversal wave which, in turn, induces a longitudinal wave, because of nonlinear geometrical coupling. The longitudinal wave travels 10 to 20 times faster than the transverse one, and thus it comes first at the bridge. The resulting variation of tension is oriented in the direction of the string. Because of the angle formed by the string with the horizontal plane, this induces a vertical component of the longitudinal force at the bridge, in addition to the transverse force. In our numerical model, the total bridge force is distributed in space in the

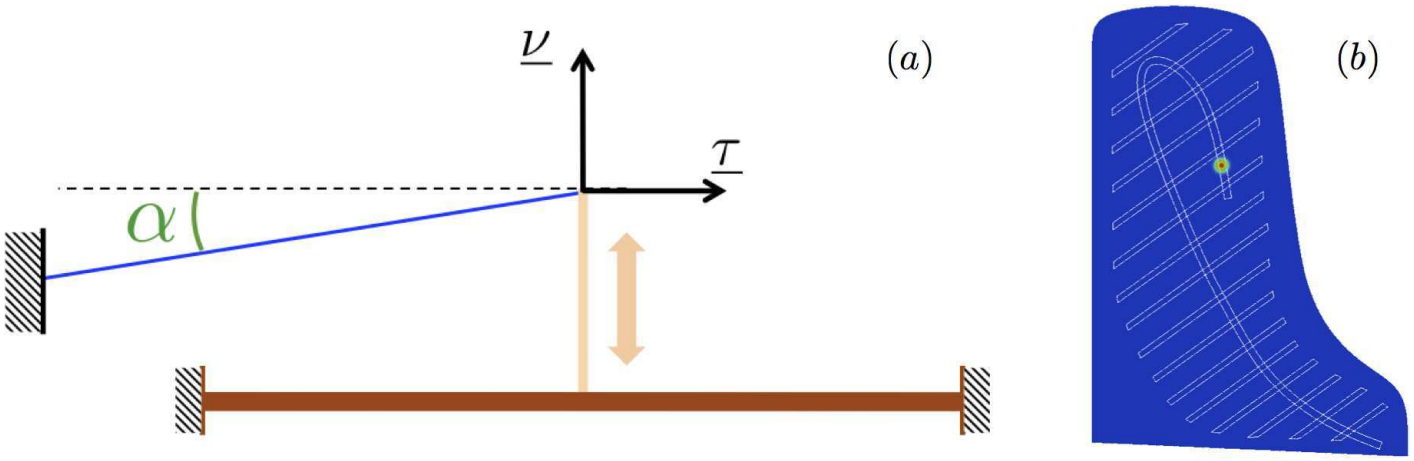

Figure 4: (a) Schematic view of strings-soundboard coupling at the bridge. The soundboard is flat because of the static action of the strings. The bridge is supposed to move in the vertical direction $\underline{\nu}$ only. The string forms a small angle α with the horizontal plane containing the vector $\underline{\tau}$. (b) Spreading function χ_ω for note C2, centered on the point where the string reaches the bridge, and rapildy decreasing.

soundboard by means of a rapidly decreasing regular function χ_ω centered on the point where the string is attached on the soundboard (see Figure 4(b)). The associated kinematic boundary conditions are the continuity of string and soundboard velocities in the vertical direction $\underline{\nu}$, and the nullity of the velocity in the horizontal direction $\underline{\tau}$ at this point (see Figure 4). These conditions are written formally:

$$\begin{pmatrix} \partial_t u_{s,i}(x=L) \\ \partial_t v_{s,i}(x=L) \end{pmatrix} \cdot \underline{\nu} = \int_\omega \partial_t u_p \, \chi_\omega, \quad \begin{pmatrix} \partial_t u_{s,i}(x=L) \\ \partial_t v_{s,i}(x=L) \end{pmatrix} \cdot \underline{\tau} = 0. \tag{18}$$

In addition, the source term in the system (14) is given by $f = -F_b(t)\,\chi_\omega(x,y)$, where $F_b(t)$ is the bridge force. Ignoring

the damping terms, and considering only one string for simplicity, this force is written:

$$F_b(t) = \cos(\alpha)\left[EA\,\partial_x u_s + AG\kappa\big(\partial_x u_s - \varphi_s\big) - (EA - T_0)\frac{\partial_x u_s}{\sqrt{(\partial_x u_s)^2 + (1+\partial_x v_s)^2}}\right](x=L,t)$$
$$+\sin(\alpha)\left[EA\,\partial_x v_s + (EA - T_0)\big(1 - \frac{1+\partial_x v_s}{\sqrt{(\partial_x u_s)^2 + (1+\partial_x v_s)^2}}\big)\right](x=L,t) \quad (19)$$

If the magnitude of the transverse motion remains small enough, it becomes justified under some conditions to derive approximate string models using an asymptotic approach [Chabassier et al., 2010]. Such models were used in the past by different authors for analytical[Bank and Sujbert, 2005] or numerical[Bilbao, 2005] purposes. In our case, we will not use this approximate system for the modeling of the piano, and the mathematical reasons for this choice were given explicitely in a previous paper [Chabassier and Joly, 2010]. However, interesting properties can be derived from the approximate expression of the bridge force:

$$F_b(t) \approx \cos(\alpha)\left[T_0\,\partial_x u_s + AG\kappa\big(\partial_x u_s - \varphi_c\big)\right.$$
$$\left.+(EA - T_0)\partial_x u_s\,\partial_x v_s + (EA - T_0)\frac{(\partial_x u_s)^3}{2}\right](x=L,t)$$
$$+\sin(\alpha)\left[EA\,\partial_x v_s + (EA - T_0)\frac{(\partial_x u_s)^2}{2}\right](x=L,t). \quad (20)$$

From Eq. (20), it can be derived that the quadratic and cubic terms in u_s generate double and triple combinations of the transverse eigenfrequencies[Bank and Sujbert, 2005]. Combination of longitudinal and transverse eigenfrequencies can also exist potentially, through the product $u_s v_s$. These combinations correspond to the so-called "phantom" partials.

2.5 Sound propagation and structural acoustics

We are now interested in the propagation of piano sounds in free space. The rim (occupying the space Ω_r) is considered to be a rigid obstacle. The acoustic velocity $\underline{V}_a$ and the acoustic pressure P are solutions of the linearized Euler equations with velocity $c_a = 340$ m/s, density $\rho_a = 1.29$ kg/m^3 and adiabatic compressibility coefficient $\mu_a = 1/(\rho_a c_a^2)$, in the unbounded domain $\Omega = \mathbb{R}^3 \setminus \{\omega \cup \Omega_r\}$ which excludes the rim and the plate:

$$\begin{cases} \rho_a \dfrac{\partial \underline{V}_a}{\partial t} + \nabla P = 0 \\ \mu_a \dfrac{\partial P}{\partial t} + \underline{\mathrm{Div}}\ \underline{V}_a = 0 \end{cases} \quad \text{in } \Omega \quad (21)$$

Viscothermal losses in the air are ignored in the acoustic model. The normal component of the acoustic velocity vanishes on the rim:

$$\underline{V}_a \cdot \underline{n}_r = 0 \qquad \text{on } \Omega_r \quad (22)$$

The coupling between the 3D sound field Ω and the vibrating soundboard ω obeys to the condition of continuity of the velocity normal components:

$$\underline{V}_a \cdot \underline{e}_z = \frac{\partial u_p}{\partial t} \qquad \text{on } \omega \quad (23)$$

where $\underline{e}_z$ completes the referential $(\underline{e}_x, \underline{e}_y)$ introduced for the describing the motion of the soundboard (see Figure 5). Finally, the soundboard force f is the pressure jump:

$$[P]_\omega = P|_{\omega^-} - P|_{\omega^+} \quad (24)$$

where ω^+ and ω^- stand for the both sides the plate. Again, the vibroacoustic system satisfies the following energy decay:

$$\frac{d\mathcal{E}_{p,a}}{dt} \leq 0 \qquad \text{with } \mathcal{E}_{p,a}(t) = \mathcal{E}_p(t) + \mathcal{E}_a(t) \quad (25)$$

where $\mathcal{E}_p(t)$ was defined in (17), and

$$\mathcal{E}_a(t) = \iiint_\Omega \frac{\rho_a}{2}\,|\underline{V}_a|^2 + \iiint_\Omega \frac{\mu_a}{2} P^2. \quad (26)$$

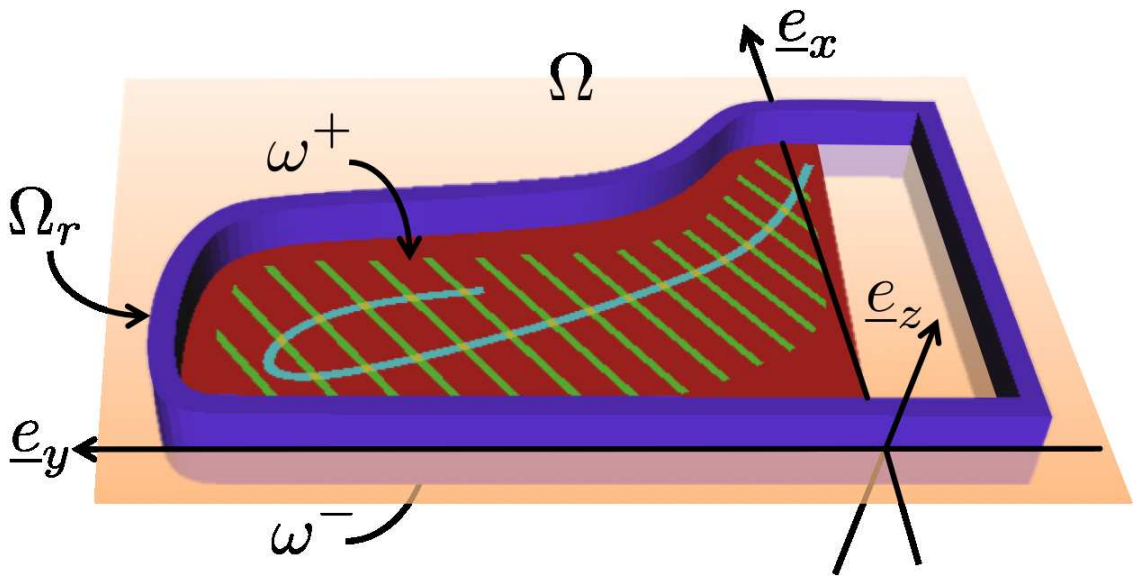

Figure 5: Geometrical configuration of the piano.

2.6 Piano model

In the complete piano model, the soundboard is coupled to the hammer – strings system, according to the description made in Section 2.4, and radiates in free space (see Section 2.5). Consequently, the force f in the system of equations (14) becomes:

$$f = -\sum_i F_{b,i}(t)\ \chi_\omega + [P]_\omega\,. \tag{27}$$

At the origin of times, the hammer has an initial velocity, while all the other parts of the system are at rest. The global coupled system satisfies the energy decay property:

$$\frac{d\mathcal{E}_{h,s,p,a}}{dt} \leq 0 \qquad \text{with } \mathcal{E}_{h,s,p,a}(t) = \mathcal{E}_{h,s}(t) + \mathcal{E}_p(t) + \mathcal{E}_a(t), \tag{28}$$

where $\mathcal{E}_{h,s}(t)$ is defined in (13), $\mathcal{E}_p(t)$ is defined in (17), and $\mathcal{E}_a(t)$ is defined in (26). In our model, it is assumed that there is no dissipation in the coupling terms. In other words, all dissipative terms are intrinsic to the constitutive elements (hammer, strings, soundboard). The acoustic dissipation is consecutive to the radiation in free space, which corresponds to energy loss for the "piano" system.

3 Numerical formulation

We now turn to the discretization of the global piano model described in the previous sections. We have to solve a complex system of coupled equations, where each subsystem has different spatial dimensions, which poses specific difficulties. The hammer-strings part is a 1D system governed by nonlinear equations. The soundboard is a 2D system with diagonal damping. The acoustic field is a 3D problem in an unbounded domain. The selection of the appropriate numerical methods are governed by the necessity of constructing an accurate and *a priori* stable scheme.

The nonlinear parts of the problem (hammer-strings interaction, string vibration), the couplings between the subsystems and, more generally, the size of the problem in terms of computational burden, requires to guarantee the long-term numerical stability. In the context of wave equations, and in musical acoustics particularly[Rhaouti et al., 1999, Derveaux et al., 2003], a classical and efficient technique to achieve this goal is to design numerical schemes based on the formulation of a discrete energy which is either constant or decreasing with time. This discrete energy has to be consistent with the continuous energy of the physical system. Ensuring the positivity of the discrete energy, then a priori estimates can be established for the unknowns of the problem leading to the stability of the method. For most numerical schemes this imposes a restriction on the discretization parameters, as, for example, an upper bound for the time step.

Another innovative aspect of our method is that the reciprocity and conservative nature of the coupling terms are guaranteed. In the discrete formulation, these couplings need a specific handling in order to guarantee a simple energy transfer, without any artificial introduction of dissipation or instabilities. Our choice here is to consider discrete coupling terms that cancel each other when computing the complete energy. In total, this method yields centered implicit couplings between the unknowns of the subsystems. The order of accuracy of the method is preserved, compared to the order of each subsystem taken independently, with no additional stability condition.

In view of the diversity of the various problems encountered in the full piano model, different discretization methods are chosen for each subsystem and for the coupling terms. The complete piano model is written in a variational form. In summary:

- High-order finite elements in space, and an innovative nonlinear three-points time discretization are used on the string,
- A centered nonlinear three time steps formulation is used for the hammer-strings coupling,
- A modal decomposition, followed by a semi-analytic time resolution is used for the soundboard,
- A centered formulation is used for the strings-soundboard coupling, where the forces acting at the bridge are introduced as additional unknowns,
- High-order finite elements in the artificially truncated space coupled to Perfectly Matched Layers, and an explicit time discretization are used for the acoustic propagation.

The numerical schemes used are not presented in detail below. We restrict the presentation to some general survey on the numerical resolution and on its main difficulties. A detailed and rigorous description of the method is given in another more numerically-oriented paper by two of the authors[Chabassier and Joly, 2012b].

3.1 Strings

Standard high-order finite elements are used for the space discretization of the nonlinear system of equations that govern the vibrations of the strings. The spatial discretization parameters (mesh size and polynomial order) are selected to ensure a small numerical dispersion in the audio range. The time discretization of the strings system is probably the most novel and innovative method used in our piano numerical formulation.

The most popular conservative schemes for wave equations are the family of θ-schemes, which have two drawbacks in the context of the piano string: firstly, they were designed for linear equations, and, secondly, the less dispersive schemes in this family are subject to a stability condition that yields an upper bound for the time step (the so-called CFL condition). Therefore, it has been decided to adopt two different discretization schemes for the linear and the nonlinear part of the system, respectively. In addition, a variation of the θ-scheme is developed for the linear part that combines both stability and accuracy.

For the nonlinear part, one major difficulty is that no existing standard scheme has the capability to preserve a discrete energy. As a consequence, we had to develop new schemes[Chabassier and Joly, 2010] based on the expression of a discrete gradient, which ensures the conservation of an energy, for a class of equations called "Hamiltonian systems of wave equation". We have shown that no explicit scheme could ensure this property, and thus the final numerical scheme is implicit in time (which implies that a nonlinear system must be solved at each time iteration). For a scalar equation, for example, the scheme would simplify treat a continuous derivative term $H'(u)$ as a quotient of the form:

$$H'(u(n\,\Delta t)) \approx \frac{H(u_h^{n+1}) - H(u_h^{n-1})}{u_h^{n+1} - u_h^{n-1}} \tag{29}$$

For the system of string equations, this method is generalized to a the gradient $\nabla H(u, v, \varphi)$.

In the linearized part of the string system, transverse, longitudinal and shear waves coexist. In the piano case, the first ones propagate much slower than the two others. In the audio range, and for the 88 notes of the instrument, small numerical dispersion must be guaranteed for the series of transverse partials and for the lowest longitudinal components. The shear components are beyond the audio range, and thus only stability conditions without too restrictive conditions in terms of dispersion are needed.

L	A	ρ	T_0	E	I	G	κ	N_x	order	Δt
m	m^2	$kg{\cdot}m^{-3}$	N	Pa	m^4	Pa	-	-	-	s
1.945	1.31×10^{-6}	44290	1328	2.02×10^{11}	1.78×10^{-14}	1.00×10^{10}	0.95	300	4	5×10^{-6}

Table 2: Parameters for the note D♯1 used in the simulations shown in Figure 6. The observation point is located at a distance of 6 cm from one end. Simply supported boundary conditions are considered.

In view of these considerations, a novel implicit discretization has been elaborated that reduces the numerical dispersion while allowing the use of a large time step in the numerical computations[Chabassier and Imperiale, 2012]. This method is based on the classical second-order time derivative centered approximation and the three points centered θ-approximation:

$$\begin{cases} \dfrac{\partial^2 u}{\partial t^2}(n\,\Delta t) \approx \dfrac{u_h^{n+1} - 2u^n + u_h^{n-1}}{\Delta t} \\ u(n\,\Delta t) \approx \theta\, u_h^{n+1} + (1-2\theta)\, u_h^n + \theta\, u_h^{n-1} \end{cases} \tag{30}$$

where $\theta \in (0, \dfrac{1}{2})$. For $\theta \geq 1/4$, the numerical scheme is unconditionally stable, while for $\theta < 1/4$ the time step must be lower than a maximal value which decreases when the wave velocity increases. A classical analysis shows that the value $\theta = 1/12$ minimizes the numerical dispersion, but choosing this value for the whole system would yield a very severe time step restriction, because of the two fastest waves. We propose a scheme where the value $\theta = 1/4$ is used for the longitudinal and shear waves, hence relaxing the stability condition, and the value $\overline{\theta} = 1/12$ for the transverse wave, hence reducing the numerical dispersion for the series of transverse partials (see figure 6). The implicit nature of the resulting scheme might be a drawback in other contexts, but is not penalizing here since an implicit scheme is already necessary for the nonlinear part of the system.

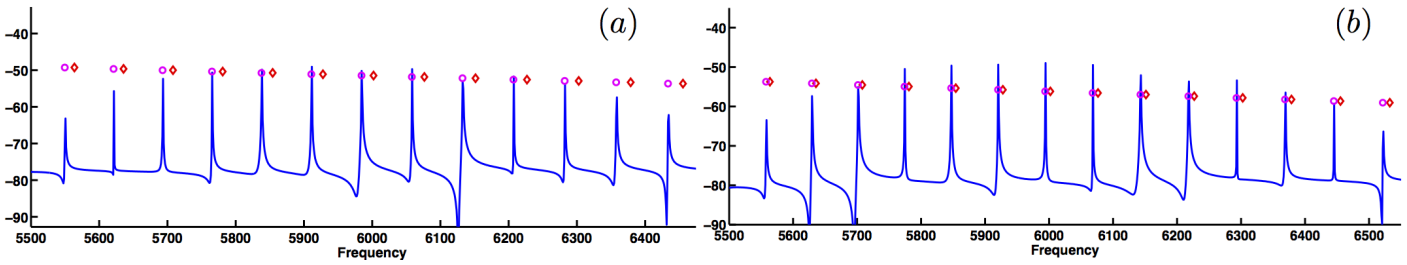

Figure 6: Spectrum of the transverse displacement of string D♯1 when considering the linear Timoshenko model. Parameters are listed in Table 2. Solid line: spectrum obtained from numerical simulation. Circle: theoretical spectrum of the numerical simulations. Diamonds: theoretical spectrum of the continuous system. (a) Usual θ-scheme, with $\theta = 1/4$. (b) New scheme with $\theta = 1/4$, $\overline{\theta} = 1/12$. The new scheme reduces the numerical dispersion, compared to the usual θ-scheme, with no computational overcost. (Color online)

In summary, the numerical scheme is a 1D nonlinear system that must be solved at each time step. The solution is computed via an iterative modified Newton-Raphson method which needs the evaluation of both the scheme and its Jacobian with respect to the unknowns. It can be shown that a discrete energy is decaying, after extinction of the source. The stability of the numerical scheme can be derived from this property, with condition on the time step. In practice, for typical space discretization parameters, a time step $\Delta t = 10^{-6}$ s yields stable and satisfying results in terms of dispersion.

3.2 Hammer-strings coupling

Since the displacement of the hammer ξ is a scalar function of time, we choose to solve the hammer-strings system by considering all together the unknowns of every strings belonging to the considered note, plus the hammer scalar unknown $\xi_h^n \approx \xi(n\,\Delta t)$.

The nonlinear hammer-strings interacting force is treated in a centered conservative way, following the ideas used for the string system (the function Φ of equation (12) is seen as the derivative of its primitive function $-\Psi$ for which we use

equation (29)). A global discrete energy is shown to be decaying with respect to time when the hammer is given with an initial velocity.

3.3 Soundboard

The soundboard model assumes a diagonal damping in the modal basis. Its motion is first decomposed onto the modes of the undamped Reissner-Mindlin system (14) belonging to the audio range, after semi-discretization in space with high-order finite elements[Derveaux et al., 2003]. In practice, 2 400 modes are needed to model the soundboard vibrations up to 10 kHz.Figure 7 shows some of the numerically computed modes associated to their eigenfrequencies. The presence of ribs and bridges is visible in the high frequency range. These modes are only computed once for all, before starting the time computation.

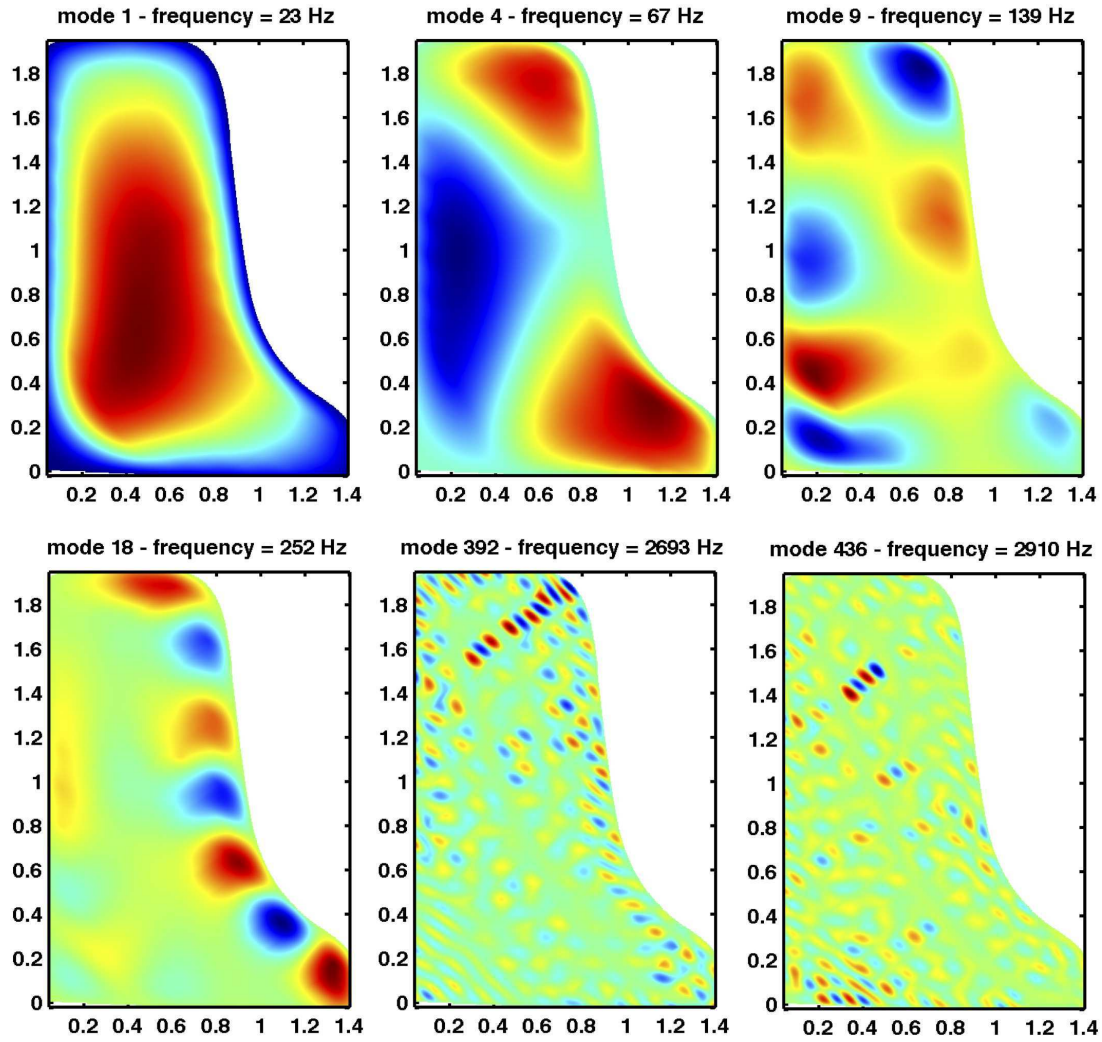

Figure 7: Examples of soundboard eigenmodes, computed with fourth-order finite elements (nearly 450 000 degrees of freedom). (Color online)

The choice of Reissner-Mindlin plate model has been validated numerically by comparison with a 3D elastodynamic computation, and, experimentally, by comparisons with measurements on rectangular plates made by other authors[Lambourg, 1997].

The discrete modal amplitudes $X_{h,n}(t)$ of the discrete eigenmodes are solutions of the uncoupled second-order equations:

$$\frac{d^2 X_{h,n}}{dt^2} + (2\pi f_{h,n})^2 X_{h,n} = F_{h,n}$$

where the $f_{h,n}$ are the numerically computed eigenfrequencies. We then introduce a discrete damping mode per mode:

$$\frac{d^2 X_{h,n}}{dt^2} + \alpha(f_{h,n})\frac{dX_{h,n}}{dt} + (2\pi f_{h,n})^2 X_{h,n} = F_{h,n} \tag{31}$$

This procedure yields decoupled equations which can be solved analytically in time, without introducing any additional approximation or numerical dispersion[Derveaux et al., 2003]. The energy identity over time of the semi-discrete problem is also exactly satisfied with this method. However, one drawback of this choice is the loss of the local nature of the couplings with strings and air.

3.4 Strings-soundboard coupling at the bridge

The discrte formulation of the strings-soundboard continuity equations must be done with special care in order to ensure the stability of the resulting coupled scheme. The purpose here is to couple the implicit three points nonlinear strings scheme described in 3.1 with the time semi-analytic soundboard model described in 3.3. Now, the last point of the string has to fulfil a discrete condition consistent with the continuity condition expressed in Eq. (18).

For computational efficiency reasons, new variables are introduced that represent the coupling forces associated to the cinematic conditions between string and soundboard expressed in Eq. (18) (see Figure 4). The strings and soundboard unknowns are evaluated on interleaved time grids: $\{n\,\Delta t\}$ for the strings, and $\{(n+1/2)\,\Delta t\}$ for the soundboard. The forces at the bridge are considered constant on time intervals of the form $[(n-1/2)\Delta t, (n+1/2)\Delta t]$. The coupling condition is an implicit version of Eq. (18) centered on times $n\,\Delta t$.

Due to the linearity of the soundboard model, it is possible to express the soundboard unknowns as linear functions of the forces at the bridge. Thanks to this property, it is possible to perform Schur complements on the system which, originally, is globally implicit. An algorithm is then writen which updates first the unknowns of the strings and the forces at the bridge, and, in a second step, updates the unknowns of the soundboard.

3.5 Acoustic propagation and structural acoustics

The acoustic domain being unbounded, it is necessary to artificially truncate the computational domain, while minimizing the wave reflection on this artificial boundary, for instance with Perfectly Matched Layers [Bécache et al, 2003]. Even after this truncation, the numerical parameters need to be chosen very small, because of the necessary wideband computation. A commonly accepted rule is to provide at least 10 points per wavelength so that the signal is spatially well sampled by the discretization. For example, if one has to model the propagation of an acoustic wave with frequency content up to 10 kHz, with a corresponding smallest wavelength of 3.4 cm, one has to provide a mesh composed of 3 mm large elements. Since the size of a piano can be 2 m large and 3 m long, with a 40 cm rim, the mesh often reaches 60 millions of degrees of freedom.

The acoustical problem is solved in space with high-order finite elements and in time with an explicit Krank-Nicholson scheme, in view of the large number of degrees of freedom to consider. The acoustic velocity $\underline{V}_{a,h}$ and pressure P_h unknowns are calculated at times $\{n\,\Delta t\}$ and $\{(n+1/2)\,\Delta t\}$, respectively. This scheme has with a stability condition: the adopted time step must be very small (around 10^{-6} s). In the variational formulation, the coupling between soundboard and air appears as source terms for the soundboard and the sound pressure equations. These terms are constructed in the discrete scheme so that they vanish when computing the energy, centered at times $n\,\Delta t$. An implicit coupling exists between the soundboard displacement and the acoustic pressure in the vicinity of the plate, which implies a change of basis between the physical and the modal representations of the soundboard. Due to the linearity of the equations, it is possible here to perform Schur complements, and to write an efficient algorithm that updates separately the plate (with a semi-analytic method) and the air variables (with the Krank-Nicholson scheme).

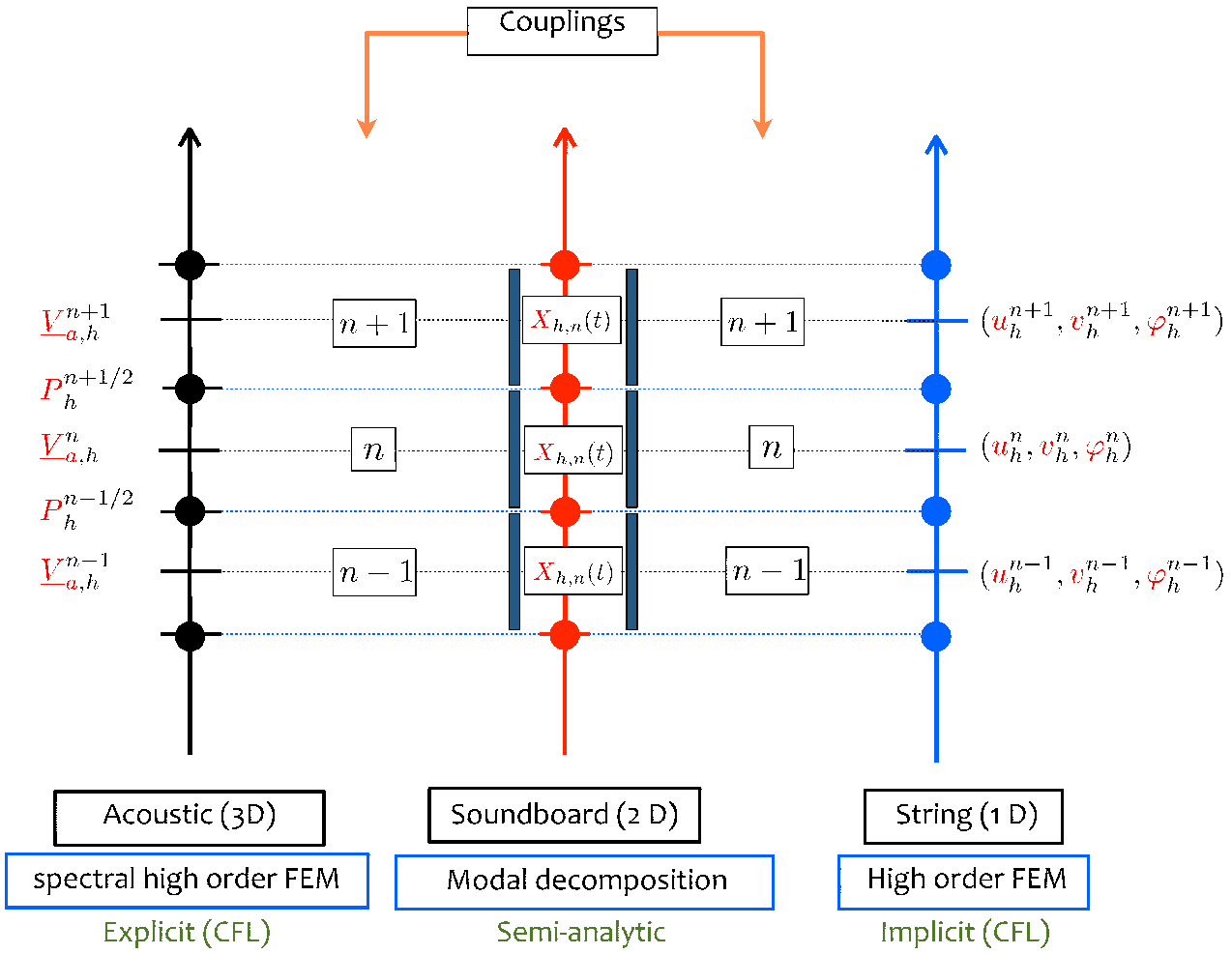

Figure 8: Schematic view of the discretization. The string's variables (u_h, v_h, φ_h) are evaluated on the time grid $\{n\,\Delta t,\ ;\ n \in \mathbb{N}\}$. The soundboard modal displacements $X_{h,p}$ are calculated at times $\{(n+1/2)\,\Delta t\}$. The acoustic velocity $\underline{V}_{a,h}$ is calculated at times $\{n\,\Delta t\}$ and the acoustic pressure P_h is calculated at times $\{(n+1/2)\,\Delta t\}$. All methods used yield energy identities, where the energies are centered on times $\{(n+1/2)\,\Delta t\}$. The coupling terms representing the forces at the bridge are centered on times $\{n\,\Delta t\}$. (Color online)

3.6 A virtual piano

The resulting numerical scheme is stable (under some conditions on the numerical parameters), globally implicit, nonlocal for the soundboard, and uses multifarious methods. The efficiency of the computer code was optimized through the use of adapted additional unknowns and Schur complements, so that the update of the unknowns of each subsystem is made separately at each time step. A massively parallelization of the code was necessary, and special attention was paid to each expensive computational step, which can significantly deteriorate the global computation time. Finally, the computation time for one second of sound of the complete piano model (with frequency content up to 10 kHz) takes one day on a 300 cpus cluster.

On figure 9 the main unknowns of the problem are represented for the note C2. nearly 3000 degrees of freedom (dofs) are used on each string of the triplet, 420 000 dofs to comput the modes of the soundboard (we only consider the 2400 first modes), and more than 90 000 000 dofs in the air. The time step is 10^{-6} second. The parameters are listed in Table 1 for the soundboard and in Table 3 for the string. The hammer strikes the strings with a velocity of 4.5 $\mathrm{m{\cdot}s^{-1}}$. The precursor can clearly be seen (in gray scale): when the longitudinal wave of the string arrives at the bridge, the soundboard is pushed down (see figure 9(b)), until the transverse wave arrives and pulls the soundboard up (see figure 9(g)). The acoustic wave is absorbed by the artificial boundary, and the rim is an obstacle to sound propagation (see figure 9(h)). Figure 10 shows

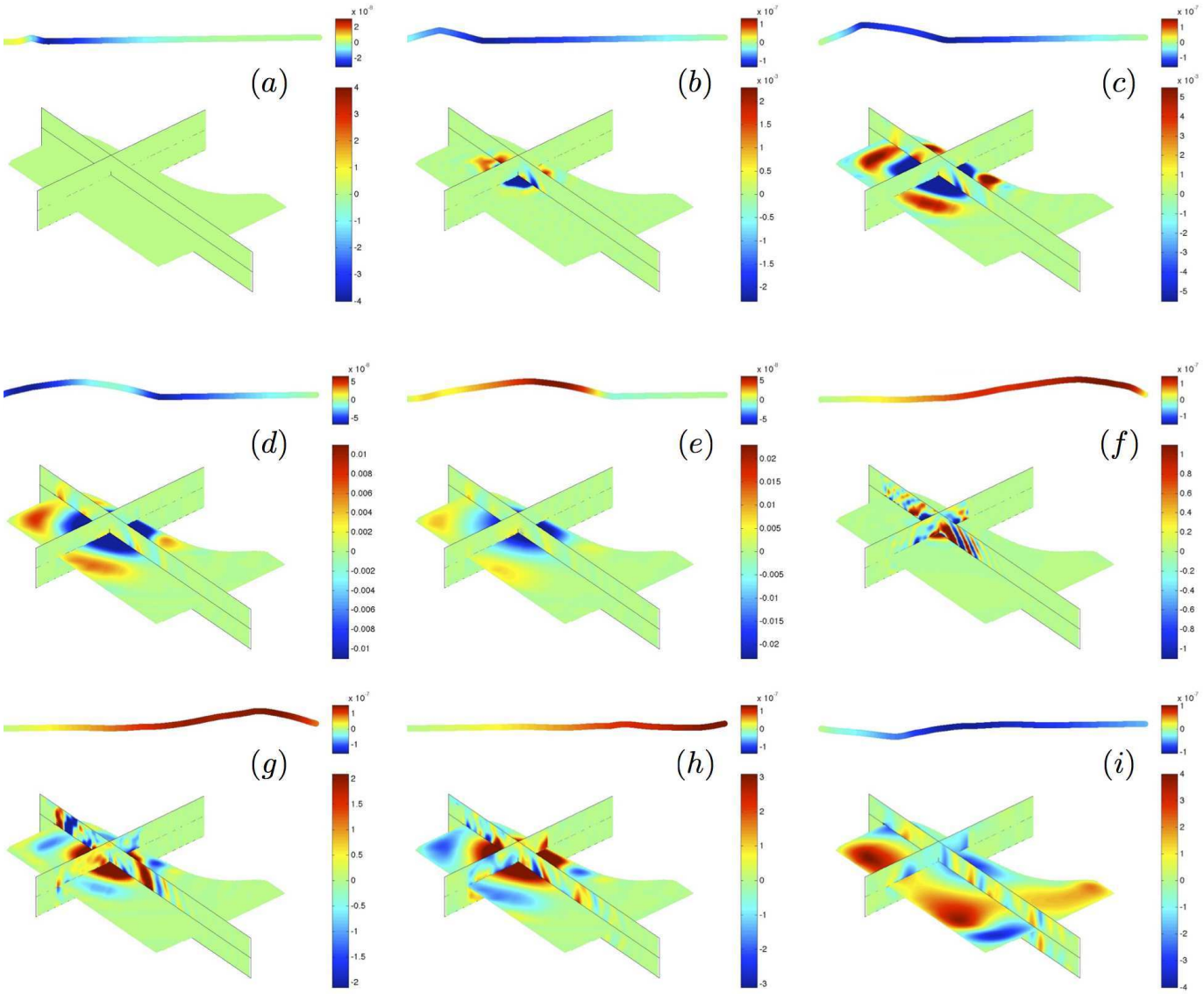

Figure 9: Time evolution of the main variables of the problem. The transverse displacement of the string is represented in the upper parts of the figures, while the longitudinal displacement is shown in color scale (color online). The displacement of the soundboard is shown in the horizontal plane in color scale (color online), while the pressure is shown in a different scale in the two vertical planes which cross at the point where the string is aatached to the bridge $x = 0.59$ m and $y = 1.26$ m. (a) $t = 0.4$ ms. (b) $t = 1.1$ ms. (c) $t = 2.1$ ms. (d) $t = 3.1$ ms. (e) $t = 4.1$ ms. (f) $t = 5.1$ ms. (g) $t = 7.1$ ms. (h) $t = 8.1$ ms. (i) $t = 16.1$ ms.

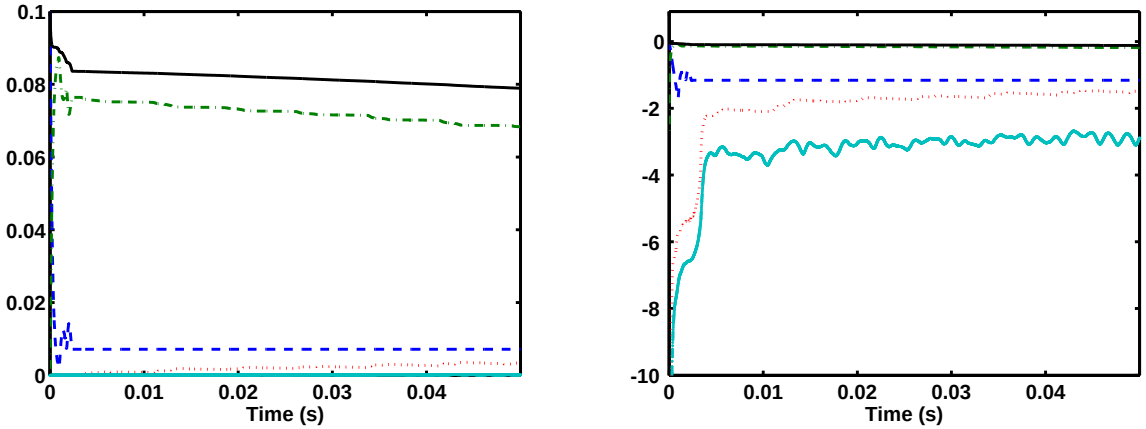

Figure 10: Energy vs time for note C2 (three strings). Solid line: Total energy. [- -] Hammer. [- ·] Strings. [···] Soundboard. [Thick -] Air. (a) Normal scale. (b) Logarithmic scale.

	Note	D♯1	C2	F3	C♯5	G6
L	(m)	1.945	1.600	0.961	0.326	0.124
d	(mm)	1.48	0.9502	1, 0525	0, 921	0.794
T_0	(N)	1781	865	774	684	587
f_0	(Hz)	38.9	65.4	174.6	555.6	1571.4
p		2.4	2.27	2.4	2.6	3.0
$K^{\mathcal{H}}$	(N·m^{-p})	4.0×10^8	2×10^9	1.0×10^9	2.8×10^{10}	2.3×10^{11}
$M^{\mathcal{H}}$	(g)	12.00	10.20	9.00	7.90	6.77
$x^{\mathcal{H}}$	(m)	0.25	0.2	0.115	0.039	0.015
x_0	(m)	0.47	0.59	0.54	0.88	1.16
y_0	(m)	1.63	1.26	0.83	0.23	0.05

$$A = \frac{\pi d^2}{4}, \quad I = \frac{\pi d^4}{64}, \quad E = 2.0 \times 10^{11} \text{ Pa}, \quad G = 8 \times 10^{10} \text{ Pa}$$

Table 3: Parameters used for the strings in the simulations

the energy evolution of each subsystem versus time, in linear and logarithmic scales. The energy associated to sound propagation is computed in the truncated domain only. The total energy (solid line) is decreasing, as expected.

4 Results of the simulations

In order to show the ability of the method to simulate the complete register of a piano, the results (output data) of the model are presented and discussed in this Section for different notes in the low (D♯1 and $C2$), medium (F3) and treble (C♯5 and G6) register, respectively.

Since the nonlinear string is one major feature of the model, particular attention is paid to the influence of string amplitude on the resulting sound. The amplitude of transverse string motion is linked to the impact velocity of the hammer. The string amplitudes of the simulated tones, normalized with respect to string diameter, and the associated hammer impact velocities are shown in Table 4. Comparisons with real tones allows to group the simulations into typical categories of touch: piano, mezzo-forte, forte, fortissimo, corresponding to realistic, though relatively arbitrary, hammer velocity ranges (ref Askenfelt Jansson).

As a rule of thumb, it is generally admitted that, for thin structures, nonlinear effects become apparent when the amplitude of the vibrations are comparable to the thickness (cite Nayfeh et Mook, chapitre 7). Transposing this rule to

Table 4: String amplitude and initial hammer velocity of the tones simulated with the present model. ADR is the maximum amplitude-to-diameter ratio of the strings.

String	ADR	Hammer velocity (m/s)	touch
D♯1	0.568	0.5	p
D♯1	1.77	1.5	mf
D♯1	3.59	3	f
C2	0.685	0.5	p
C2	2.01	1.5	mf
C2	4.05	3	f
F3	0.337	0.5	p
F3	1.04	1.5	mf
F3	2.10	3	f
C♯5	0.274	0.5	p
C♯5	0.87	1.5	mf
C♯5	1.76	3	f
C♯5	2.64	4.5	ff
G6	0.12	0.5	p
G6	0.443	1.5	mf
G6	0.96	3	f

the case of strings yields the condition $ADR = \frac{|u_s|}{d_s} > 1$, where d_s is the diameter of the string. According to this rule, Table 4 predicts that nonlinear effects should be noticeable in the bass and medium ranges, even for moderate hammer velocity, whereas they should be less easily detectable for the treble notes except for strong impacts. This simple criterion is in accordance with experimental observations.

The order of the presentation follows the course of energy transmission in the piano: from hammer to strings, from bridge to soundboard, and from soundboard to air. The input parameter is the initial velocity of the hammer at the time where it comes in contact with the strings. The present model ignores the action of key mechanism prior to this contact.

To illustrate this, Figure 11 shows measured and simulated starting transients for the note D♯1. One can see the successive transformations of the hammer pulse to string wave, bridge and soundboard accelerations, and sound pressure. These waveforms and they corresponding spectra will be analyzed and discussed throughout the paper.

An essential requirement for piano tone modeling is the accuracy of frequency estimation. To illustrate this feature, Figure 12 shows an example of string spectrum for the note D♯1 (7th string with fundamental 39 Hz). Both measured and simulated string's eigenfrequencies strictly follow the stiffness dispersion curve predicted by the Timoshenko model, at least up to the 60th partial (around 3 kHz). Precise measurements on partials of lower amplitude are difficult beyond this limit, because of noise and blurred spectral content.

One effect of string nonlinearity is the dependence of frequency with amplitude. For the note C♯5 played forte, for example, Figure 13 shows that the frequency of the fundamental decreases with time, a consequence of amplitude decrease due to damping.

Observations made on real signals show that the pressure and soundboard motion spectra, including the bridge, have a more dense and rich content than the strings. The simulations help here to understand these differences and identify the additional spectral components. In the low-frequency range, most of the additional spectral peaks correspond to soundboard modes excited by the string pulse. These modes are particularly visible for the upper keys of the piano, because of large spacing between the strings' partials (see Figure 14). The presence of soundboard modes in sound pressure and soundboard motion is a result of a linear coupling with the strings and thus, there are present in the spectrum even for light hammer touch. These modes are damped more rapidly than the string's partials, and thus they are essentially audible during the initial transients of the tones.

Increasing the hammer velocity progressively induces additional peaks between the string components, a consequence of string nonlinearity and coupling at the bridge. As explained in Section 2, a coupling exists between transverse and longitudinal motion of the nonlinear string. Due to the string-bridge coupling conditions, both these transverse and

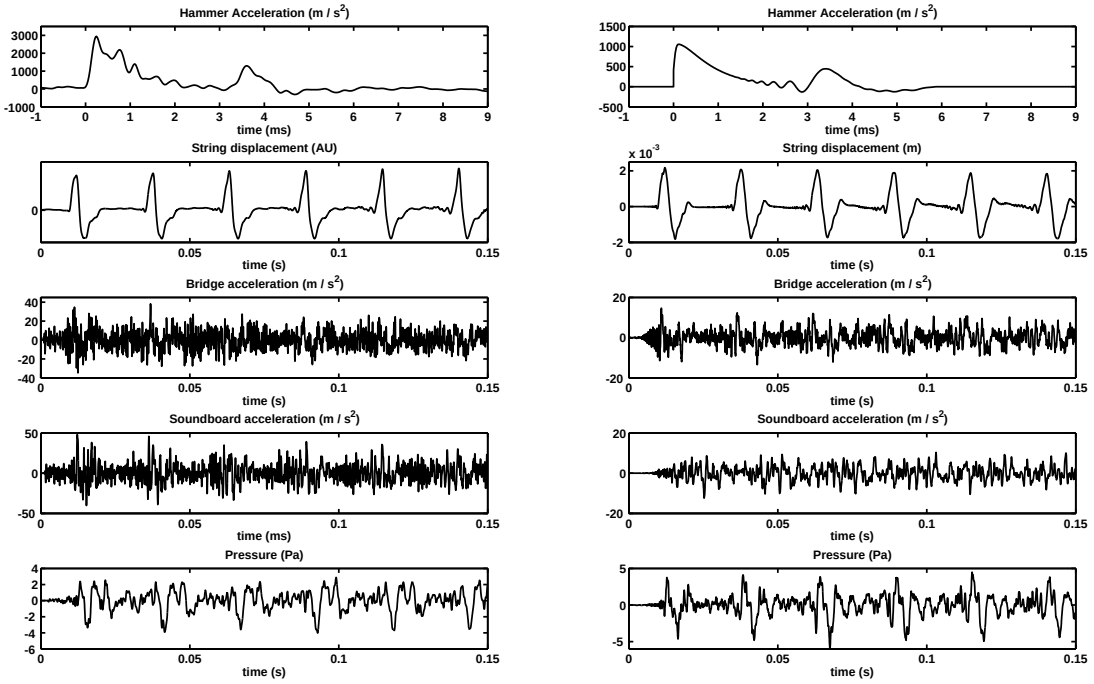

Figure 11: Measured (left) and simulated (right) starting transients of the main variables for note D♯1 (7th). From top to bottom: hammer acceleration, string displacement (at point located 1.749 m from the agraffe), bridge acceleration at string end, soundboard acceleration (at point x=0.17 m ; y=1.49 m in the coordinate axes shown in Fig. 3), sound pressure (simulated at point x=0.8500 ; y=1.4590 ; z=0.3800, measured in the nearfield at a comparable location).

longitudinal components are transmitted to the soundboard. This explains why the longitudinal eigenfrequencies of the strings are visible on bridge and soundboard waveforms, but not on the transverse string motion (voir ref Podlesak et Giordano ?). In addition, a consequence of the nonlinear terms in the string wave equation is that combinations of string components are created: the so-called "phantom partials" (Conklin99).

As explained theoretically from Eq. 20 in Section 2, the frequencies of these phantoms correspond to sums (or differences) between two or three of the string components, depending on whether the combinations are the results of quadratic, or cubic, nonlinearities. In general, all combinations are not observable and obey to complex rules. The instability conditions that gives rise to these components must reach a certain threshold (Watzky ? Bank ?, Nayfeh). Such analysis is beyond the scope of this paper. Notice in Figure 15 that the frequencies predicted by sums or differences of partials'eigenfrequencies correspond with great accuracy (less than 1 Hz) to the observed phantoms, both in simulations and measurements. Similar phenomena are observed in gongs and cymbals (Chaigne, Touz).

In the time-domain, the presence of nonlinear coupling is seen in the precursors. Fig. 11 shows that the precursor is not visible on the string displacement, while it is clearly seen on the other waveforms (bridge, soundboard, pressure), both in measurements and simulations. This precursor is primarily due to the longitudinal waves which travel faster than the transverse waves along the string. In real instruments, the composition of these precursors is more complex and not totally elucidated (see Askenfelt). Presumably, they content some signature of shock of the key on the keybed and other structural components that are not included in our model.

One further interest of simulations lies in the possibility of separating phenomena that are intrinsically linked in the reality. In this respect, damping factors and decay times of the partials are good illustrating examples. When systems are coupled, it is always problematic to separate the causes of losses. In contrast, a model has the capability of introducing dissipation of energy in the hammer felt, along the string, and at the ends, separately. Even more interesting

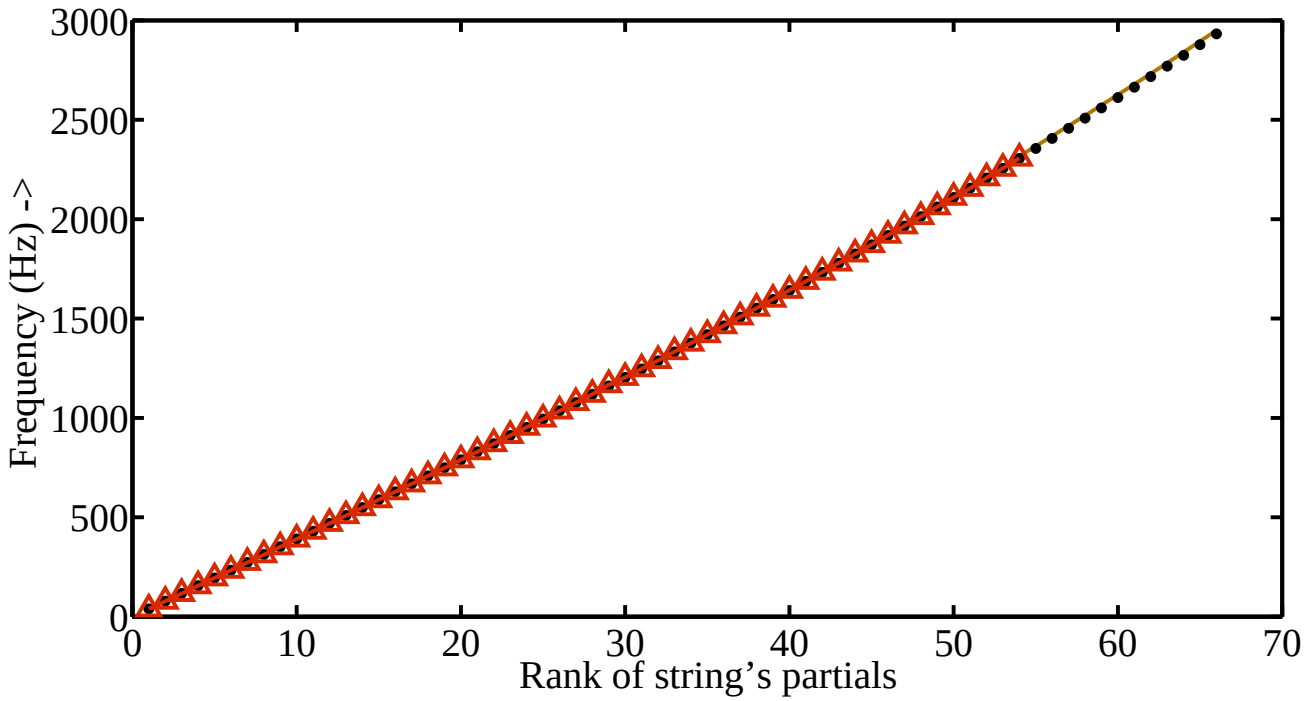

Figure 12: Comparison between the string's eigenfrequencies derived from frequency analysis of the simulated (black circles) and measured (triangles) string spectra, and the theoretical dispersion curve predicted by the Timoshenko model (solid line). Note D♯1. (Color online).

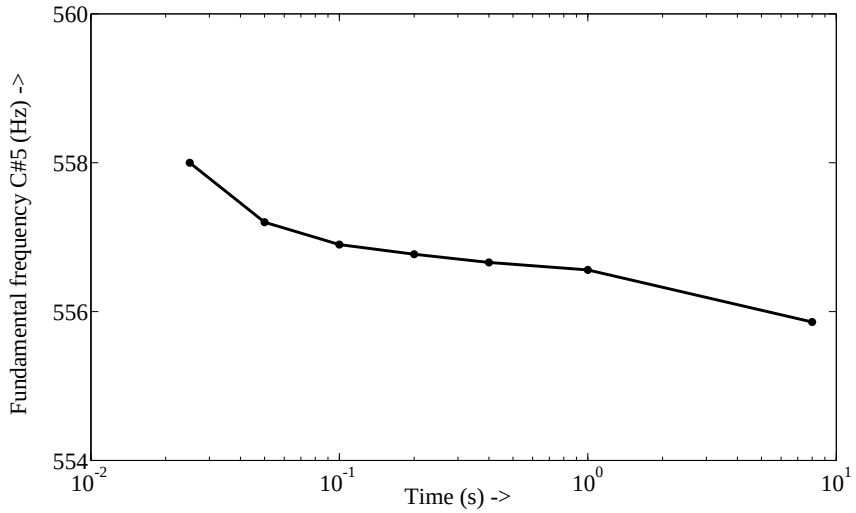

Figure 13: Evolution of frequency with time of the fundamental, due to geometrical nonlinearity. Simulation of note C♯5 played fortissimo.

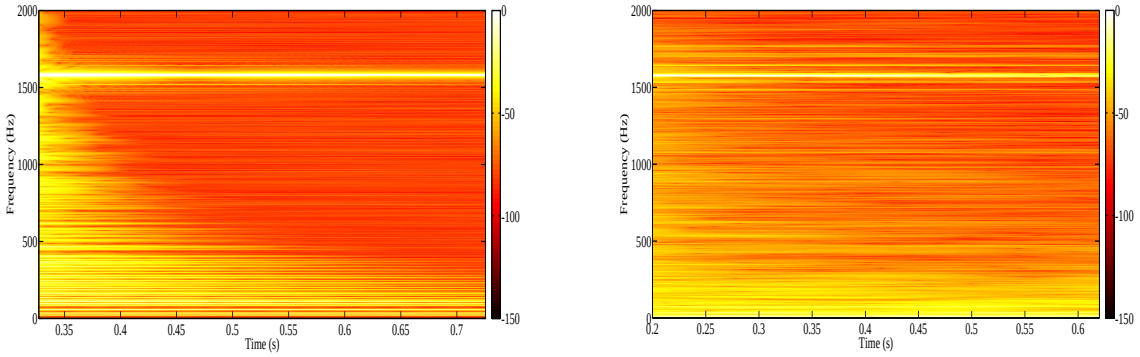

Figure 14: Comparison between simulated (left) and measured (right) G6 spectrum, below the fundamental, showing a large density of soundboard modes. (Color online)

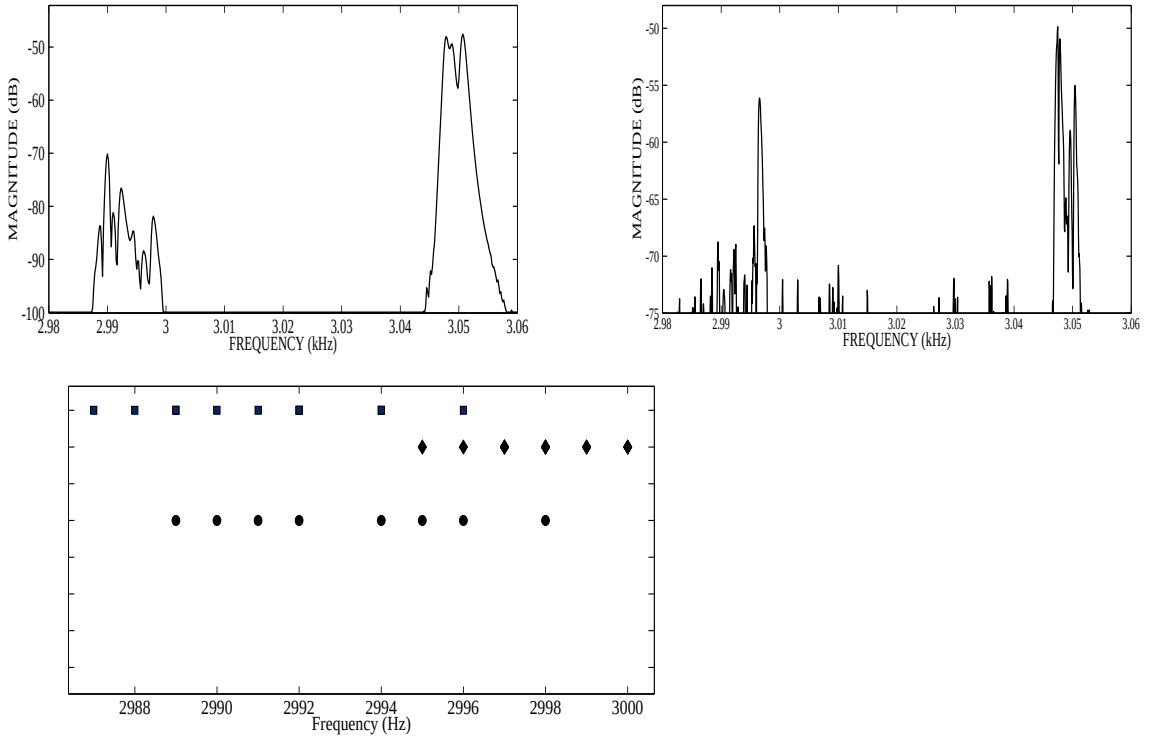

Figure 15: (Top) Comparison between simulated (left) and measured (right) F3 spectrum near the 17th partial (3.05 kHz), showing the presence of phantom partials between 2.99 and 3.0 kHz. (Bottom) Accurate measurements of phantom frequencies on the simulated F3 tone (circles). Comparison with sums (diamonds) and differences (squares) of the frequencies of strings' partials.

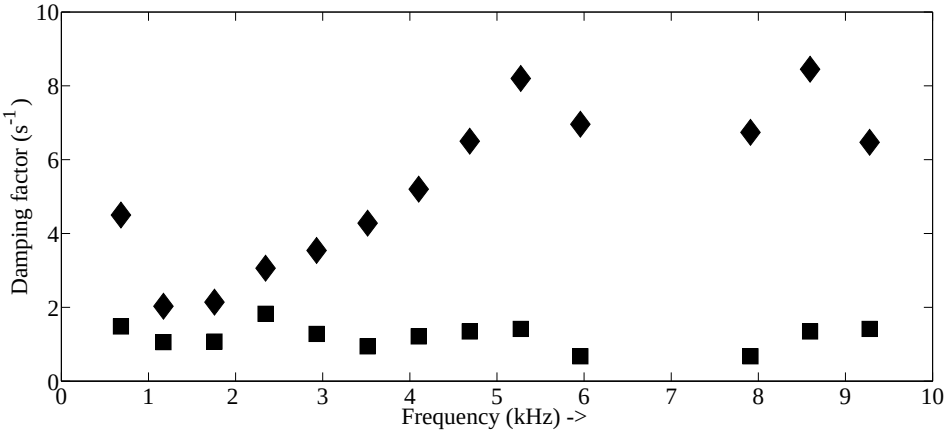

Figure 16: Damping factors of the partials due to radiation (squares) and for all causes of losses (diamonds). Simulations of note C♯5.

is the separation of structural and radiation losses in the soundboard. Experimentally, such a separation requires a rather delicate procedure where the instrument has to be put in a vacuum chamber in order to modify the conditions of radiation (see David). One difficulty of these experiments follows from the modifications of wood properties consecutive to variations of ambient pressure, and thus investigating such a problem with the help of simulations is an appealing alternative. To illustrate this ability of the model, Fig. 16 shows the damping factors derived from simulations for the C♯5 note, for radiation losses only, compared to the damping factors obtained when introducing losses in various parts of the instrument (hammer felt, string, soundboard, radiation).

5 Conclusion

In this paper, a global model of a grand piano has been presented. This model couples together the hammer, the nonlinear strings, the soundboard with ribs and bridges, and the radiation of acoustic waves in free field. As far as we are aware, this is probably the most general physical model of a piano available today. However, a number of significant features of real pianos were not considered in this model. The key mechanism, and an accurate description of the hammer action including the vibrations of the hammer shank, have been left aside. From the point of view of the player, adding this part would certainly allow interesting studies of the links between the action of the finger and the resulting sound.

Beside this, a great improvement of the string model would be to account for the nonplanar motions observed on real pianos. A strong hypothesis is that this motion might be due to the generally observed zig-zag clamping conditions at the bridge (ref Stuart), but this needs to be verified and quantified by careful measurements. To reproduce such effects, more appropriate boundary conditions have to be developed, that allow the progressive transformation of a vertical polarization into an horizontal motion. The way both polarizations are then transmitted to the rest of the structure also need to be better understood. It turns out that the coexistence of these polarizations with different decay times greatly influence the amplitude envelope of the tone, and thus its perception.

The motion of the structure is restricted here to the soundboard. Previous measurements (ref Askenfelt 93) tend to show that some other parts of the instrument contribute to the sound. In this context, it would be attractive to reproduce the shock of the key against the keybed and the vibrations of the rim, to evaluate their relevance.

The present model is solved in the time-domain. The results yield the temporal evolution of the main significant variables of the system simultaneously: hammer force, string motion, bridge and soundboard vibrations, pressure field. The obtained waveforms can be heard through headphones or loudspeakers, and clearly evoke piano tones. They also shed useful light on the transfer of energy and transformations of the signals from hammer to strings, soundboard and air.

To solve the problem, specific and original numerical methods were developed for each part of the piano. A gradient approach coupled to high order finite elements lead us to design an energy decaying numerical scheme for the string's system, which is nonlinearly coupled to the hammer. A modal method was chosen to solve the soundboard problem, with a diagonal damping form. The eigenmodes and eigenfrequencies are computed once for all using high order finite elements

method, and an analytic formula is then discretized in time. Finally, sound radiation is solved with finite difference in time and high order finite elements in the space domain, which is artificially truncated with PML (Perfectly Matched Layers).

As a result, a numerical formulation of the global piano model is obtained with high precision in time, space and frequency. This formulation ensures that the total energy of the system is conserved. The model accounts for the dependence of piano sounds and vibrations with amplitude, due to nonlinear modeling of strings and hammers. In this respect, the simulations show the main effects of nonlinearity observed on real tones: precursors, time evolution of eigenfrequencies, transverse-longitudinal coupling, and phantom partials. The model used for string-soundboard coupling at the bridge is consistent with the transmission of nonlinearities observed on real instruments. Due to this coupling, the presence of the soundboard modes in the piano transients are reproduced in a natural way. The soundboard model also integrates the presence of ribs and bridges, which are treated as heterogeneities in material and thickness of a Reissner-Mindlin plate.

The piano is a instrument with a large register. Most of the notes, from bass to treble, show a wideband spectrum, with significant energy up to 10 kHz and more. As a consequence, piano modeling requires a fine spatial grid for each part. The most demanding grid is associated with the modeling of the pressure field. This part of the simulations was a particular challenging point of the work, which necessitated high performance parallel computing. In the present state of the equipment, several hours of computation in parallel on a 300 cpus cluster are necessary to compute the pressure field during one second in a box of the order of 10 m^3 that contains the instrument[Chabassier and Durufle, 2012].

Analysis of the simulated piano tones in time and frequency show a satisfactory agreement with measurements performed on a Steinway D grand piano. This particular instrument was used for extracting accurate values of input parameters, thus allowing precise comparisons between model and measurements for some selected notes in the bass, medium and treble range. Informal auditory evaluation of the simulated tones indicates that medium and treble notes are fairly well reproduced, but that the depth of the bass notes is not completely rendered.

In its present state, this model of piano should be considered as a crude skeleton of the instrument. Its prime function is to get a better understanding of the complex coupled phenomena involved in a complete piano, with the possibility of systematic variations of some selected parameters that are not conceivable in the reality. Numerous additional improvements, careful adjustments and fine tuning would be necessary before thinking of competing with high-quality pianos. However, even in its imperfect form, we believe that the model could be used as a companion tool for piano making. In this context, investigating the influence of soundboard modifications on the radiation of sound and on string-bridge coupling appear as potentially fruitful examples.

6 Acknowledgment

Simulations presented in this paper were carried out using the PLAFRIM experimental testbed, being developed under the Inria PlaFRIM development action with support from LABRI and IMB and other entities: Conseil Régional d'Aquitaine, FeDER, Université de Bordeaux and CNRS (see https://plafrim.bordeaux.inria.fr/) and the computing facilities MCIA (Mésocentre de Calcul Intensif Aquitain) of the Université de Bordeaux and of the Université de Pau et des Pays de l'Adour (see http://www.mcia.univ-bordeaux.fr).

References

[Askenfelt, 1993] Askenfelt, A. (1993). Observations on the transient components of the piano tone. STL-QPSR, 34(4):15–22.

[Balmes, 2006] Balmes, E. (2006). Modeling damping at the material and structure level. In Proceedings of the 24th IMAC Conference and exposition on structural dynamics, 3:1314–39.

[Bank and Lehtonen, 2010] Bank, B. and Lehtonen, H.-M. (2010). Perception of longitudinal components in piano string vibrations. J. Acoust. Soc. Am., 128(3):EL117–EL123.

[Bank and Sujbert, 2005] Bank, B. and Sujbert, L. (2005). Generation of longitudinal vibrations in piano strings: From physics to sound synthesis. J. Acoust. Soc. Am., 117(4):2268–2278.

[Bensa et al., 2003] Bensa, J., Bilbao, S., and Kronland-Martinet, R. (2003). The simulation of piano string vibration: from physical models to finite difference schemes and digital waveguides. J. Acoust. Soc. Am., 114(2):1095—1107.

[Bilbao, 2005] Bilbao, S. (2005). Conservative numerical methods for nonlinear strings. J. Acoust. Soc. Am., 118(5):3316–3327.

[Bilhuber and Johnson, 1940] Bilhuber, P. H. and Johnson, C. A. (1940). The influence of the soundboard on piano tone quality. J. Acoust. Soc. Am., 11(3):311–320.

[Chabassier et al., 2010] Chabassier, J., Chaigne, A., and Joly, P. (2010). Transitoires de piano et non linéarités des cordes : mesures et simulations. Proceedings of the 10th French Acoustical Society Meeting (in french).

[Chabassier and Durufle, 2012] Chabassier, J. and Durufle, M. (2012). Physical parameters for piano modeling. Inria Technical Report No 0425.

[Chabassier and Imperiale, 2012] Chabassier, J. and Imperiale, S. (2012). Stability and dispersion analysis of improved time discretization for simply supported prestressed Timoshenko systems. Application to the stiff piano string. Wave Motion, to appear, doi 10.1016/j.wavemoti.2012.11.002.

[Chabassier and Joly, 2010] Chabassier, J. and Joly, P. (2010). Energy preserving schemes for nonlinear Hamiltonian systems of wave equations. Application to the vibrating piano string. Computer Methods in Applied Mechanics and Engineering, 199:2779–2795.

[Chabassier et al., 2012a] Chabassier, J. and Chaigne, A. and Joly, P. (2012). Time domain simulation of a piano. Part I: model description. Inria Research Report , No 8097.

[Chabassier and Joly, 2012b] Chabassier, J. and Joly, P. (2012b). Time domain simulation of a piano. Part II : numerical aspects. Math. Model. Numer. Anal., in preparation.

[Chaigne and Askenfelt, 1994] Chaigne, A. and Askenfelt, A. (1994). Numerical simulation of piano strings I. A physical model for a struck string using finite-difference methods. J. Acoust. Soc. Am., 95(2):1112–1118.

[Cohen and Grob, 2007] Cohen, G. and Grob, P. (2007). Mixed higher order spectral finite elements for Reissner–Mindlin equations. Siam J. Sci. Comput., 29(3):986.

[Cuenca and Caussé, 2007] Cuenca, J. and Caussé, R. (2007). Three-dimensional interaction between strings, bridge and soundboard in modern piano's treble range. 19th international congress on acoustics, pp 1–6.

[Derveaux et al., 2003] Derveaux, G., Chaigne, A., Joly, P., and Bécache, E. (2003). Time-domain simulation of a guitar: Model and method. J. Acoust. Soc. Am., 114(6):3368–3383.

[Ege, 2012] Ege, K., X. Boutillon and M. Rébillat (2012). Vibroacoustics of the piano soundboard: (Non)linearity and modal properties in the low- and mid- frequency ranges. J. Sound Vib., doi http://dx.doi.org/10.1016/j.jsv.2012.10.012.

[Fletcher, 1964] Fletcher, H. (1964). Normal vibration frequencies of a stiff piano string. J. Acoust. Soc. Am., 36(1):203–209.

[Giordano and II, 2000] Giordano, N. and II, J. W. (2000). Piano hammers and their force compression characteristics: does a power law make sense? J. Acoust. Soc. Am., 107(4):2248–2255.

[Giordano and Jiang, 2004] Giordano, N. and Jiang, M. (2004). Physical modeling of the piano. Eurasip Journal on Applied Signal Processing, 7:926–933.

[Giordano and Korty, 1996] Giordano, N. and Korty, A. J. (1996). Motion of a piano string: Longitudinal vibrations and the role of the bridge. J. Acoust. Soc. Am., 100(6):3899–3908.

[Harold A. Conklin, 1996a] Harold A. Conklin, J. (1996a). Design and tone in the mechanoacoustic piano. Part II. Piano structure. J. Acoust. Soc. Am., 100(2):695–708.

[Harold A. Conklin, 1996b] Harold A. Conklin, J. (1996b). Design and tone in the mechanoacoustic piano. part iii. piano strings and scale design. J. Acoust. Soc. Am., 100(3):1286–1298.

[Harold A. Conklin, 1997] Harold A. Conklin, J. (1997). Piano strings and "phantom" partials. J. Acoust. Soc. Am., 102(1):659–659.

[Harold A. Conklin, 1999] Harold A. Conklin, J. (1999). Generation of partials due to nonlinear mixing in a stringed instrument. J. Acoust. Soc. Am., 105(1):536–545.

[Hasselman, 1976] Hasselman, T. K. (1976). Modal coupling in lightly damped structures. AIAA Journal, 14:1627–28.

[Bécache et al, 2003] E. Bécache, S. Fauqueux, and P. Joly (2003). Stability of perfectly matched layers, group velocities and anisotropic waves. Journal of Computational Physics, 188:399403.

[Jarvelainen et al., 2001] Jarvelainen, H., Valimaki, V., and Karjalainen, M. (2001). Audibility of the timbral effects of inharmonicity in stringed instrument tones. Acoustics Research Letters Online, 2(3):79–84.

[Lambourg, 1997] Lambourg, C. (1997). Modèle temporel pour la simulation numérique de plaques vibrantes - Application à la synthèse sonore. PhD thesis, Université du Maine.

[Mamou-Mani et al., 2008] Mamou-Mani, A., Frelat, J., and Besnainou, C. (2008). Numerical simulation of a piano soundboard under downbearing. J. Acoust. Soc. Am., 123(4):2401–2406.

[Morse and Ingard, 1968] Morse, P. and Ingard, K. (1968). Theoretical Acoustics.

[Podlesak and Lee, 1988] Podlesak, M. and Lee, A. R. (1988). Dispersion of waves in piano strings. J. Acoust. Soc. Am., 83(1):305–317.

[Rhaouti et al., 1999] Rhaouti, L., Chaigne, A., and Joly, P. (1999). Time-domain modeling and numerical simulation of a kettledrum. J. Acoust. Soc. Am., 105(6):3545–3562.

[Stulov, 2004] Stulov, A. (2004). Dynamic behavior and mechanical features of wool felt. Acta Mechanica, 169(1):13–21.

[Weinreich, 1977] Weinreich, G. (1977). Coupled piano strings. J. Acoust. Soc. Am., 62(6):1474–1484.

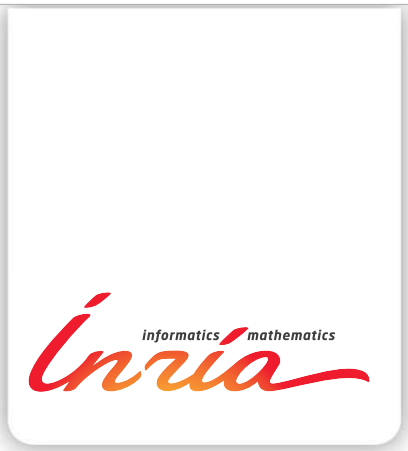

RESEARCH CENTRE
BORDEAUX – SUD-OUEST

200 Avenue de la Vieille Tour,
33405 Talence Cedex

Publisher
Inria
Domaine de Voluceau - Rocquencourt
BP 105 - 78153 Le Chesnay Cedex
inria.fr

ISSN 0249-6399